fixed evolution HETCOR sequences (refs 6 and 7), and Professor David Coker for assistance in the molecular modeling.

Supplementary Material Available: Clavudiol (1), ^1H and ^{13}C one-dimensional spectra, DQCOSY, long-range COSY (Δ = 300 ms), HETCOR, FLOCK two-dimensional NMR spectra, and CD spectrum; clavirolide A (2) ^1H and ^{13}C one-dimensional spectra, COSY, long-range COSY (Δ = 300 ms), RCT, fixed-evolution HETCOR, and FLOCK two-dimensional spectra; tables of final atomic coordinates, noteworthy bond distances, bond angles, and atomic thermal parameters; and perspective drawing from crystallographic study of 1 (31 pages). Ordering information is given on any current masthead page.

New Briarein Diterpenes from the Caribbean Gorgonians *Erythropodium caribaeorum* and *Briareum* sp.

Evamarie O. Pordesimo, Francis J. Schmitz,* Leon S. Ciereszko, M. Bilayet Hossain, and Dick van der Helm*

Department of Chemistry and Biochemistry, University of Oklahoma, Norman, Oklahoma 73019

Received July 23, 1990

Seven new erythrolides (3–9) and the known briarein diterpenes erythrolide A (1) and erythrolide B (2) have been isolated from the gorgonian *Erythropodium caribaeorum* collected in the U.S. Virgin Islands and Jamaica. A *Briareum* sp. of gorgonian yielded nine new briarein diterpenes (10–18), which have been named briareolides. The structures of these compounds were determined by spectroscopic methods, especially one- and two-dimensional NMR. The structure and absolute stereochemistry of briareolide B (11) was determined by X-ray crystallographic analysis. Some of the briareolides have displayed antiinflammatory activity.

A large number of diterpenes that have the briarein skeleton typified by briarein A[1,2] (I) have been isolated from gorgonians,[3-13] sea pens,[14-16] and a soft coral[17] within the past 15 years. Diterpene metabolites of this type continue to intrigue investigators because of the structural novelty and complexity and interesting biological activity (e.g., insecticidal, antiinflammatory, antiviral) associated with several of these compounds.

We report here our investigation of the extracts from the gorgonians *Erythropodium caribaeorum* from the U.S. Virgin Islands and Jamaica and a species of *Briareum* from Puerto Rico. The known compounds erythrolide A[6] (1)

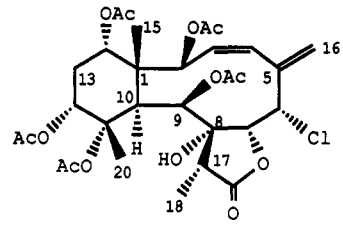

I

and erythrolide B[6] (2) were isolated from *E. caribaeorum* along with seven new erythrolides, compounds 3–9. The *Briareum* sp. (identified as either *B. asbestinum* or *B. polyanthes*) yielded nine new briarein type compounds 10–18, which were named briareolides.

Results and Discussion

Isolation and Structure Determination of Erythrolides from *E. caribaeorum*. The erythrolides were isolated by conventional methods as outlined in the Experimental Section. Erythrolide A (1)[6] and erythrolide B(2)[6] were identified by comparison of their ^1H NMR spectra with those reported in the literature. The ^1H NMR spectrum of 2 obtained at 20 °C in $CDCl_3$ contained some broadened signals which were sharpened considerably at 58 °C. This suggested the existence of slowly interconverting conformers for this compound. A 2D ^1H NMR homonuclear correlation experiment (COSY) allowed the assignment of all the signals in the ^1H NMR spectrum of 2, including those overlapped in the region from 5.0 to 5.7 ppm. The OH signal assignment (δ 2.71) was confirmed by exchange with CD_3OD.

Compound 3, named erythrolide C according to the nomenclature used by Look and Fenical,[6] was isolated from a fraction that was slightly less polar than the fraction containing erythrolide B (2). A molecular formula of $C_{24}H_{29}O_9Cl$, estimated from ^1H and ^{13}C NMR data, was confirmed for 3 by high-resolution FAB$^+$ mass spectrometry. The intensity of the M + 2 isotope peak observed in the low-resolution FAB$^+$ mass spectrum [(M + H +

(1) Burks, J. E.; van der Helm, D.; Chang, C. Y.; Ciereszko, L. S. *Acta Crystallogr.* **1977**, *B33*, 704.
(2) Bartholome, C. Ph.D. Dissertation, Universite Libre de Bruxelles, 1974.
(3) Chang, C. Y. Ph.D. Dissertation, University of Oklahoma, Norman, OK, 1977.
(4) Stierle, D. B.; Carte, B.; Faulkner, D. J.; Tagle, B.; Clardy, J. *J. Org. Chem.* **1980**, *102*, 5088.
(5) Look, S. A. Ph.D. Dissertation, University of California, San Diego, 1983.
(6) Look, S. A.; Fenical, W.; Van Engen, D.; Clardy, J. *J. Am. Chem. Soc.* **1984**, *106*, 5026.
(7) Grode, S. H.; James, T. R.; Cardellina, J. H., II; Onan, K. D. *J. Org. Chem.* **1983**, *48*, 5203.
(8) Grode, S. H.; James, T. R.; Cardellina, J. H., II. *Tetrahedron Lett.* **1983**, *24*, 691.
(9) Cardellina, J. H., II; James, T. R.; Chen, M. H. M.; Clardy, J. *J. Org. Chem.* **1984**, *49*, 3398.
(10) Vasilescu, I. Ph.D. Dissertation, James Cook University of North Queensland, Townesville, Australia.
(11) Bloor, S. J. B. Ph.D. Dissertation, University of Oklahoma, Norman, OK, 1986.
(12) Bowden, B. G.; Coll, J. C.; Patalinghug, W.; Skelton, B. W.; Vasilescu, I.; White, A. H. *Aust. J. Chem.* **1987**, *40*, 2085.
(13) Groweiss, A.; Look, S. A.; Fenical, W. *J. Org. Chem.* **1988**, *53*, 2401.
(14) Wratten, S. J.; Fenical, W.; Faulkner, D. J.; Wekell, J. C. *Tetrahedron Lett.* **1977**, 1559.
(15) Wratten, S. J.; Faulkner, D. J.; Hirotsu, K.; Clardy, J. *J. Am. Chem. Soc.* **1977**, *99*, 2824.
(16) Hendrickson, R. L.; Cardellina, J. H., II. *Tetrahedron Lett.* **1986**, 6565.
(17) Ksebati, M. B.; Schmitz, F. J. *Bull. Soc. Chim. Belg.* **1986**, *95*, 835–851.

0022-3263/91/1956-2344$02.50/0 © 1991 American Chemical Society

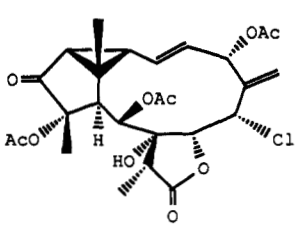

1 Erythrolide A[6]

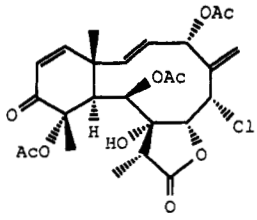

2 Erythrolide B[6]

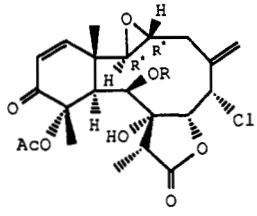

3 Erythrolide C, R = Ac
4 Erythrolide D, R = $(CO)CH_2O(CO)CH_3$

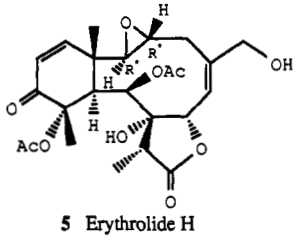

5 Erythrolide H

2)$^+$/(M + H)$^+$ = 0.39] and the occurrence of a fragment ion corresponding to $M^+ - 35$ were strong indications of the presence of a chlorine atom in **3**. The infrared spectrum of **3** contained absorptions for hydroxyl (3540 cm^{-1}), γ-lactone (1780 cm^{-1}), ester (1735 cm^{-1}), and enone (1685 cm^{-1}) functionalities, the same structural features found in erythrolide B (**2**). The enone functionality was also supported by a UV absorption at λ_{max} (MeOH) 215 (ϵ 8910). Comparison of the ^1H and ^{13}C NMR spectra of **3** (see Tables I and III) with those of erythrolide B confirmed the structural similarity of these two compounds and revealed the presence of some features unique to **3**. The γ-lactone moiety and the functionality in the six-membered ring of **2** (i.e., α,β-unsaturated ketone and acetate group) were assumed to be intact in **3** on the basis of similar IR, UV, and NMR data (compare signals of related H's and C's in Tables I and III). Erythrolide C (**3**), however, had only two acetate groups (vs three in erythrolide B) as indicated by ^1H signals at δ 2.16 (3 H, s) and 2.06 (3 H, s) and ^{13}C signals at δ 169.4 (s) and 169.2 (s). Also, resonances at δ 62.1 (d) and 53.9 (d) in the ^{13}C NMR spectrum of **3** indicated the presence in this compound of an epoxide moiety,[18] a feature not found in **2**.

The partial structures for **3** shown in Figure 1 were deduced from ^1H NMR spin decoupling and COSY experiments. Chemical shifts of the protonated carbons were assigned by a 2D ^1H–^{13}C heterocorrelation experiment (HETCOR,[19] J = 140 Hz). Partial structures A and B, and most of C above, were reminiscent of those in erythrolide B (**2**). Unique to erythrolide C (**3**) was the segment shown in the boxed section of partial structure C. Allylic coupling between one of the exocyclic olefinic protons (δ 5.12) and one of the methylene proton signals (δ 2.77) was observed in the COSY spectrum. The signal at δ 4.78 was likewise shown by COSY to be coupled to both of the exocyclic olefinic methylene protons, and also to the methine proton at δ 5.20.

The gross structure of erythrolide C shown in Figure 2 was obtained by piecing together all the above partial structures based on long-range ^1H coupling and NOE information. *W*-couplings were observed between the ring junction methyl signal at δ 1.13 (Me-15) and each of the proton signals at δ 3.08 (H-2) and 4.08 (H-10). The latter

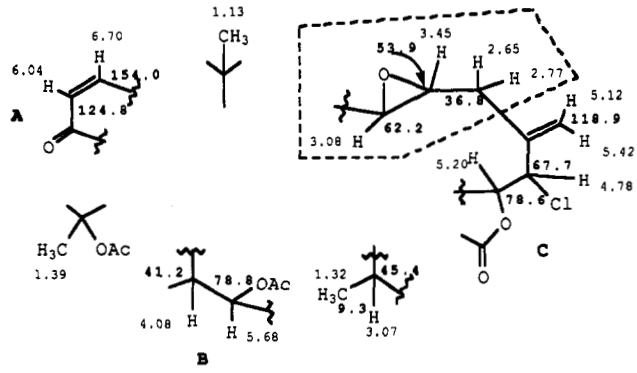

Figure 1. Partial structures for erythrolide C (**3**).

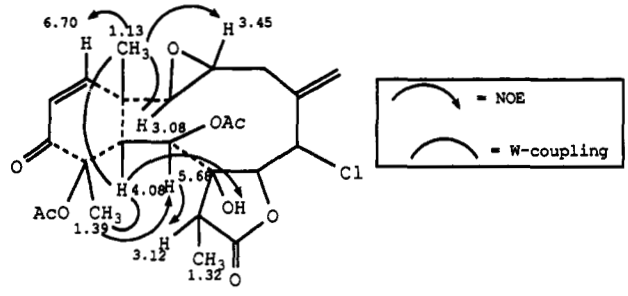

Figure 2. *W*-Couplings and NOEs in erythrolide C (**3**).

signal was also *W*-coupled to the methyl signal at δ 1.39 (Me-20). An NOE enhancement of the doublet signal at δ 6.70 (H-14) was observed upon irradiation of the Me-15 signal. These data established the connectivity as well as the trans stereochemistry at the ring juncture. Other NOEs observed for **3** are given in Table IV. After arbitrary assignment of the ring juncture methyl as being on the β face, the 2,3-epoxide was also determined to be β on the basis of an NOE between the H-10 and H-2 signals. Enhancement of the signal for H-3 (δ 3.45) upon irradiation of the Me-15 signal placed the former on the β face as well. Assignment of H-7 (δ 5.20) as β followed from its NOE with H-3. The small coupling (1.4 Hz) observed between H-6 (δ 4.78) and H-7 (δ 5.21) suggested a near orthogonal orientation of these two protons. From examination of a Dreiding model, this would be consistent with H-6 being on the same face of the molecule as H-7. This was supported by the NOE observed between these two signals. Enhancement of the OH proton signal upon irradiation of the signal for H-10 placed the OH group on the α face. The orientation of the Me-18 group (δ 1.32) was also assigned as α because of its NOE enhancement upon irradiation of the OH proton. Irradiation of the Me-20 signal resulted in enhancement of the signal for H-9. Irradiation of this latter signal in turn resulted in enhancement of the methine quartet signal (H-17, δ 3.12). This NOE interaction between H-9 and H-17 provided experimental evidence for the C-8–C-9 bond. From examination of a Dreiding model, these protons and those of Me-20 were found to be reasonably close to each other when the C-9 acetate group was β-oriented. This completed the stereochemical analysis and structure elucidation of compound **3**. The only connection left without direct experimental evidence was that between C-11 and C-12. As predicted on the basis of the similarities in their ^1H and ^{13}C NMR data, the relative stereochemistry in erythrolide C (**3**) was identical with that in erythrolide B (**2**).

Acetylation of erythrolide C using a standard reagent (Ac_2O–pyridine), even with prolonged reaction times and higher temperatures, resulted only in recovery of starting material. The OH proton also resisted attempts to ex-

(18) Silverstein, R. M.; Bassler, G. C.; Morrill, R. C. *Spectrometric Identification of Organic Compounds*, 4th ed.; Wiley: New York, 1981.
(19) (a) Bax, A. *J. Magn. Reson.* **1983**, *53*, 517. (b) Bax, A.; Morris, G. A. *J. Magn. Reson.* **1981**, *42*, 501.

Table I. ^{1}H NMR Data for Compounds 2–5[a]

H at carbon	compound 2	3	4	5
2	6.21 (1 H, d, 15.3)	3.08 (1 H, br s)	3.08 (1 H, br s)	2.77 (1 H, d, 2.9)
3	5.62 (1 H, br d, 15.3)	3.46 (1 H, m)	3.43 (1 H, m)	3.51 (1 H, ddd, 5.8, 2.9, 2.4)
4	5.68 (1 H, d, 2.3)	2.78 (1 H, dd, 14.9, 4.98)	2.77 (1 H, 33, 14.7, 6.0)	2.93 (1 H, dd, 17.0, 5.8)
		2.65 (1 H, dd, 14.9, 3.7)	2.59 (1 H, 33, 14.7, 3.0)	2.18 (1 H, dd, 17.0, 2.4)
6	5.56 (1 H, br s)	4.79 (1 H, br s)	4.78 (1 H, br s)	5.54 (1 H, br d, 10.2)
7	5.04 (1 H, br s)	5.21 (1 H, d, 1.4)	5.14 (1 H, d, 2.1)	5.20 (1 H, d, 10.2)
9	5.51 (1 H, br s)	5.66 (1 H, br s)	5.75 (1 H, br s)	5.68 (1 H, d, 3.5)
10	3.85 (1 H, br s)	4.08 (1 H, br s)	4.12 (1 H, br s)	3.59 (1 H, d, 3.5)
13	6.07 (1 H, d, 10.2)	6.04 (1 H, d, 10.0)	6.05 (1 H, d, 10.2)	5.96 (1 H, d, 10.5)
14	6.58 (1 H, d, 10.2)	6.70 (1 H, d, 10.0)	6.67 (1 H, d, 10.2)	6.68 (1 H, d, 10.5)
15	1.43 (3 H, s)	1.14 (3 H, s)	1.13 (3 H, s)	0.94 (3 H, s)
16	5.58 (1 H, s)	5.42 (1 H, br s)	5.41 (1 H, br s)	3.95 (1 H, d, 17.0)
	5.59 (1 H, s)	5.12 (1 H, br s)	5.12 (1 H, s)	4.04 (1 H, d, 17.0)
17	2.84 (1 H, q, 7.8)	3.12 (1 H, d, 7.5)	3.01 (1 H, d, 7.5)	2.49 (1 H, q, 7.2)
18	1.27 (3 H, d, 7.8)	1.32 (3 H, d, 7.5)	1.32 (3 H, d, 7.5)	1.23 (3 H, d, 7.2)
20	1.42 (3 H, s)	1.39 (3 H, s)	1.40 (3 H, s)	1.48 (3 H, s)
acetate	2.16 (3 H, s)	2.16 (3 H, s)	2.13 (3 H, s)	2.23 (3 H, s)
methyl	2.10 (3 H, s)	2.06 (3 H, s)	2.04 (3 H, s)	2.04 (3 H, s)
	1.97 (3 H, s)			
8-OH	2.71 (1 H, br s) exch in benzene-d_6 with CD_3OD	3.16 (1 H, br s) exch in $CDCl_3$ with TFA-d	3.22 (1 H, br s) exch in $CDCl_3$ with CD_3OD	4.71
$(CO)OCH_2$	–	–	4.62 (1 H, d, 15.9)	
			4.52 (1 H, d, 15.9)	

[a] Spectra recorded in $CDCl_3$ at 300 MHz. Values reported in parts per million relative to internal TMS.

Table II. ^{1}H NMR Data for Compounds 6–9[a]

H at carbon	compound 6	7	8	9
2	4.19 (1 H, d, 1.5)	4.19 (1 H, d, 1.8)	4.21 (1 H, d, 1.98)	4.08 (1 H, br s)
3	3.97 (1 H, m)	3.97 (1 H, m)	3.97 (1 H, m)	3.86 (1 H, dt, 11, 1.4)
4	2.75 (2 H, m)	2.80 (1 H, dd, 14.7, 4.9)	2.78 (1 H, dd, 15.5, 5.0)	2.76 (1 H, dd, 15.4, <1)
		2.69 (1 H, dd, 14.7, 3.4)	2.69 (1 H, dd, 15.5, 4.0)	2.69 (1 H, dd, 15.4, <1)
6	4.79 (1 H, br s)	4.77 (1 H, br s)	4.80 (1 H, br s)	4.83 (1 H, br s)
7	4.37 (1 H, br s)	4.40 (1 H, br s)	4.37 (1 H, br s)	4.44 (1 H, s)
9	5.73 (1 H, d, 2.1)	5.81 (1 H, d, 2.1)	5.86 (1 H, d, 2.1)	6.16 (1 H, d, 2.4)
10	3.22 (1 H, d, 2.1)	3.26 (1 H, d, 2.1)	3.28 (1 H, d, 2.1)	2.30 (1 H, d, 2.4)
12	–	–	–	5.71 (1 H, d, 5.4)
13	6.00 (1 H, d, 10.2)	6.01 (1 H, d, 10.2)	6.02 (1 H, d, 10.2)	5.87 (1 H, dd, 9.9, 5.4)
14	6.65 (1 H, d, 10.2)	6.66 (1 H, d, 10.2)	6.66 (1 H, d, 10.2)	5.77 (1 H, d, 9.9)
15	1.63 (3 H, s)	1.59 (3 H, s)	1.62 (3 H, s)	1.60 (3 H, s)
16	5.67 (1 H, br s)	5.70 (1 H, br s)	5.68 (1 H, br s)	5.70 (1 H, br s)
	5.40 (1 H, br s)	5.42 (1 H, br s)	5.42 (1 H, br s)	5.40 (1 H, br s)
17	2.68 (1 H, q, 6.9)	2.65 (1 H, q, 7.2)	2.69 (1 H, q, 7.0)	2.83 (1 H, q, 6.9)
18	1.06 (3 H, d, 6.9)	1.05 (3 H, d, 7.2)	1.07 (3 H, d, 7.0)	1.20 (3 H, d. 6.9)
20	1.46 (3 H, s)	1.47 (3 H, s)	1.45 (3 H, s)	1.51 (3 H, s)
acetate	2.26 (3 H, s)	2.19 (3 H, s)	2.15 (3 H, s)	2.23 (3 H, s)
methyl	2.12 (3 H, s)	2.12 (3 H, s)		2.05 (3 H, s)
				2.00 (3 H, s)
3-OH	2.70 (1 H, d) exch with CD_3OD		2.73 (1 H, br s)	2.86 (1 H, br s)
$(CO)OCH_2$		4.72 (2 H, AB q)	4.35 (2 H, br s)	

[a] Spectra recorded in $CDCl_3$ at 300 MHz. Values reported in parts per million relative to internal TMS.

change with addition of CD_3OD and D_2O. It was only observed to exchange upon addition of TFA-d_1. These observations were consistent with the tertiary nature and sterically hindered location of the alcohol function as indicated in the proposed structure for erythrolide C (**3**).

The signal for the ring juncture proton (H-10) in **3** occurred at δ 4.08, at noticeably lower field than the values reported (δ 3–3.4) for other known briarein-type compounds of comparable structure. Apparently, the conformation imposed on the 10-membered ring by the presence of the 2,3-epoxide in compound **3** is such that H-10 is deshielded by the hydroxyl oxygen on C-8.

Erythrolide D (**4**) was present in the same fraction as erythrolide B and could only be obtained free of the latter by HPLC separation using a cyanopropyl-bonded column (hexane–2-propanol, 2:1). Separation could not be achieved with C-18 (MeOH–H_2O) nor silica gel (acetone–hexane) HPLC. High-resolution mass spectrometry established a molecular formula for **4** of $C_{26}H_{31}O_{11}Cl$, two carbon, two hydrogen, and two oxygen atoms more than in the molecular formula of erythrolide C (**3**). Like **3**, compound **4** showed IR absorptions (3540, 1775, 1745, and 1685 cm^{-1}) that indicated the presence of OH, γ-lactone, ester, and α,β-unsaturated ketone functionalities. The ^{1}H NMR spectrum of **4** was almost identical with that of **3** (see Table I), except for having an additional two-proton isolated A,B quartet spin system (δ 4.52, 4.62). Likewise, the ^{13}C NMR spectra of **3** and **4** were nearly identical, the only major difference being the presence of additional resonances in the spectrum of **4** at δ 167.0 (s) and 60.7 (t). These NMR data suggested the presence in **4** of an acetoxyacetyl group [$OC(O)CH_2OC(O)CH_3$]. Additional evi-

Table III. ^{13}C NMR Data for Compounds 2–9[a]

carbon	compound 2	3[b]	4[b]	5	6	7[b]	8[c]	9
1	41.8 (s)	40.8 (s)	40.7 (s)	40.9 (s)	36.2 (2)	36.2 (s)	36.2 (s)	35.8 (2)
2	144.5 (d)	62.2 (d)	63.0 (d)	63.9 (d)	86.2 (d)	86.3 (d)	86.2 (d)	88.0 (d)
3	131.5 (d)	53.9 (d)	53.8 (d)	57.5 (d)	69.9 (d)	70.2 (d)	70.0 (d)	69.7 (d)
4	73.5 (d)	36.8 (t)	36.9 (t)	28.6 (t)	41.2 (t)	41.3 (t)	41.2 (t)	41.4 (t)
5	141.5 (s)	137.5 (s)	137.5 (s)	147.5 (s)	138.3 (s)	138.4 (s)	138.2 (s)	138.7 (s)
6	65.7 (d)	67.7 (d)	67.6 (d)	118.3 (d)	59.3 (d)	59.3 (d)	59.3 (d)	59.1 (d)
7	79.1 (d)	78.6 (d)	78.7 (d)	69.2 (d)	85.6 (d)	85.5 (d)	85.5 (d)	85.9 (d)
8	81.0 (s)	80.0 (s)	80.0 (s)	81.9 (s)	83.1 (s)	83.0 (s)	82.9 (s)	83.3 (s)
9	77.6 (d)	78.8 (d)	78.7 (d)	78.7 (d)	68.8 (d)	69.9 (d)	69.8 (d)	68.2 (d)
10	44.9 (d)	41.2 (d)	41.4 (d)	41.2 (d)	41.6 (d)	41.8 (d)	41.8 (d)	41.4 (d)
11	80.6 (s)	81.5 (s)	81.6 (s)	81.9 (s)	80.6 (s)	80.5 (s)	80.5 (s)	83.3 (s)
12	195.5 (s)	194.0 (s)	194.7 (s)	195.2 (s)	194.1 (s)	194.0 (s)	193.9 (s)	76.5 (d)
13	126.1 (d)	124.8 (d)	124.3 (d)	124.0 (d)	124.5 (d)	124.6 (d)	124.5 (d)	120.7 (d)
14	154.5 (d)	154.0 (d)	153.7 (d)	154.3 (d)	152.4 (d)	152.3 (d)	152.4 (d)	138.3 (d)
15	22.9 (q)	16.2 (q)	16.2 (1)	14.4 (q)	21.2 (q)	20.9 (q)	21.1 (q)	21.7 (q)
16	115.5 (t)	118.9 (t)	119.0 (t)	66.5 (t)	123.0 (t)	123.0 (t)	123.0 (t)	122.9 (t)
17	48.8 (d)	45.5 (d)	45.4 (d)	43.8 (d)	48.9 (d)	49.1 (d)	49.0 (d)	49.6 (d)
18	9.3 (q)	9.3 (q)	9.1 (q)	6.9 (1)	6.6 (1)	6.6 (q)	6.6 (q)	6.3 (q)
19	176.2 (s)	175.0 (s)	175.5 (s)	176.2 (s)	174.1 (s)	174.0 (s)	173.9 (s)	174.2 (s)
20	20.7 (q)	21.3 (q)	21.2 (q)	21.6 (q)	22.3 (q)	22.3 (q)	22.3 (q)	19.4 (q)
acetate	169.5 (s)	169.4 (s)	169.2 (s)	171.2 (s)	169.9 (s)	170.0 (s)	169.9 (s)	169.8 (s)
	21.0 (q)	21.2 (q)	21.2 (q)	21.5 (q)	21.1 (q)	21.1 (q)	21.1 (q)	21.2 (q)
	169.5 (s)	169.2 (s)	170.1 (s)	169.1 (s)	169.9 (s)	170.0 (s)		169.0 (s)
	21.0 (q)	21.2 (q)	20.2 (q)	21.4 (q)	21.2 (q)	20.3 (q)		20.6 (q)
	168.9 (q)							169.0 (s)
	21.0 (q)							20.2 (q)
O(CO)CH			167.0 (s)			167.5 (s)	172.1 (s)	
			60.7 (t)			60.5 (t)	61.1 (t)	

[a] Spectra recorded in $CDCl_3$ at 75 MHz. Multiplicities obtained from DEPT experiment unless otherwise specified. [b] Assignments made from HETCOR experiment (J = 140 Hz) and/or INAPT. [c] Assignment by analogy with model compounds.

Table IV. NOE Data for Erythrolides C–I (3–9)

irr signal	enhanced signal (%) 3	4	5	6	7	8	9
H-3	H-7 (13.7), Me-15 (3.5)	H-7 (13), Me-15 (2.7), H-6 (4.1)		H-14 (9.4)		H-14 (8)	H-6 (7)
H-6				H-7 (9.7)		H-7 (2.1)	H-7 (12.8)
H-7	H-6, H-17	H-6 (4.1), Me-15 (2.7)	H-17 (4.8)				
H-9	H-17 (4), H-7 (8.4)	H-17 (21), H-10 (4.9)	H-17, H-10 (3.5)	H-17 (15.8), H-10 (9.8)	H-17 (7.5)		H-17 (14.5), Me-20 (2.8)
H-10	H-2 (14), H-9 (5.4), (OH)	H-2 (17), H-9 (4.9), OH (4)	H-2 (8.2), H-9 (2.5)	H-2, H-9 (8.6)	H-2 (7)	H-2 (11.7), H-9 (11)	H-9 (2.2)
H-14				H-13 (17.5), H-2 (8.8)		H-13 (8.4)	
Me-15	H-14 (10), H-3 (14)	H-14 (10.4), H-3 (9)	H-14 (3.5), H-3 (7.8)	H-14 (7), H-3 (8), H-6 (10)	H-14 (5.7), H-6 (9.4)	H-14 (9), H-3 (10.4), H-6 (16.4)	H-14 (4)
Me-18		OH (14.3)		H-10 (10.6)	H-10 (7)		
Me-20	H-9 (9)	H-9 (8)	H-9 (6)	H-9 (2.5)		H-9 (4.8)	H-12 (13.5), H-13 (5.4)
8-OH	H-10 (20), Me-18 (4.5)	H-10 (15.6), Me-18 (3)	H-10 (6), Me-18 (3.5), H-6 (12)				

dence for this functionality was provided in the low-resolution mass spectrum of 4 by a base peak at m/z 101 corresponding to the ion fragment, $^{+}O{\equiv}CCH_2O(CO)CH_3$. The site of attachment of this group was determined by a long-range HETCOR experiment (J = 10 Hz) to be at C-9. Thus one of the carbonyl carbon resonances, δ 167.0, showed long-range correlations with both H-9 (δ 5.75, identified by its coupling to H-10) and the methylene protons of the A,B quartet system. The latter in turn were coupled with the acetate carbonyl carbon at δ 169.2.

NOEs observed for erythrolide D (4) were similar to those in 3 as shown in Table IV.

Erythrolide E (6) was obtained only as a trace impurity of compound 3 in the Virgin Islands collection of the octocoral, but was a major constituent in the Jamaican specimens. High-resolution mass spectrometry established a molecular formula of $C_{24}H_{29}O_9Cl$ for this compound, making it isomeric with erythrolide C. The IR spectrum of 6 indicated that this compound contained the same functional group as 3, i.e., hydroxyl, γ-lactone, ester, and enone. It was initially thought that erythrolide E was merely a stereoisomer of 3 since the two compounds appeared to have the same skeletal arrangement and oxygenation pattern judging from ^1H homodecoupling, COSY, and NOE data. There were, however, significantly large differences in both ^1H and ^{13}C chemical shift values at several positions in 6 when compared to 3 (see Tables I–III) that suggested that erythrolide E was structurally different from erythrolide C. Acetylation of 6 yielded compound 19, whose ^1H NMR spectrum differed from that of starting material in having an additional acetate methyl signal at δ 2.11 and in the occurrence of the H-3 signal (identified

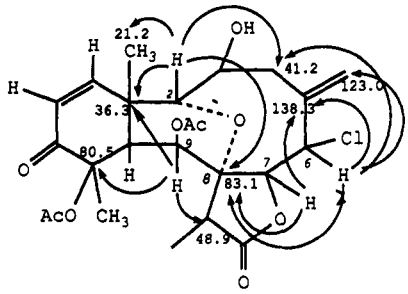

Figure 3. Long-range ^1H–^{13}C correlations for erythrolide E (**6**).

from its coupling with the H-2 and H-4 protons) at δ 5.20, ca. 1.4 ppm downfield from the value in the spectrum of **6**. This was consistent with acetylation of a hydroxyl

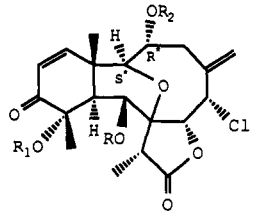

6 Erythrolide E, R = R_1 = Ac; R_2 = H

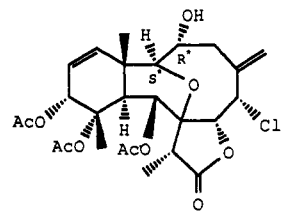

9 Erythrolide G

7 Erythrolide F, R = $(CO)CH_2O(CO)CH_3$
R_1 = Ac; R_2 = H

8 Erythrolide I, R = $(CO)CH_2OH$;
= Ac; R_2 = H

19 Erythrolide E-3-Acetate, R = R_1 = R_2 = Ac

20 Erythrolide F-3-Acetate, R = $(CO)CH_2O(CO)CH_3$
R_1 = R_2 = Ac

group. Clearly erythrolide E contained a hydroxyl group at C-3 rather than an epoxide as in metabolites **3** and **4**. To accommodate the nine degrees of unsaturation as well as the number of oxygen atoms required by the molecular formula of **6**, another ring had to be incorporated into the structure. It was thus proposed that an ether link occurred across the 10-membered ring between C-2 and C-8 (see Figure 3). This concept was supported by the NOEs observed for **6** (see Table IV), particularly those between H-14 and both H-2 and H-3, which correlated with a Dreiding model representing the relative stereochemistry shown in the structure of **6**. This was also a logical structure from a biosynthetic viewpoint. Erythrolide C (**3**) could be envisioned as a precursor for erythrolide E (or vice versa) via epoxide ring opening by an internal nucleophile, in this case the C-8 hydroxyl group. The structure of **6** was eventually confirmed through a selective INEPT[20] (or INAPT) experiment (J = 6 Hz) wherein the coupling between H-2 and C-8 was clearly demonstrated. Other pertinent ^1H–^{13}C correlations obtained from INAPT are also illustrated in Figure 3. Almost all two- and three-bond ^1H–^{13}C couplings were observed with this technique.

Compound **7**, erythrolide F, was deduced to be the C-9 acetoxyacetate analogue of **6**. This compound exhibited ^1H and ^{13}C NMR spectra nearly identical with those of **6** (see Tables II and III), the only difference being the presence in its ^1H NMR spectrum of resonances associated with the acetoxyacetyl function previously described for compound **4**. As in **4**, the presence of this group in **7** was confirmed in the low-resolution mass spectrum by an ion fragment at m/e 101 which was also the base peak. Complete ^1H and ^{13}C NMR chemical shift assignments for **7** were obtained by HETCOR and long-range HETCOR experiments. The A,B quartet protons of the acetoxyacetyl group were shown to be long-range coupled to two carbonyl carbons at δ 170.0 and 167.5. The latter was shown to be also coupled to H-9. The site of attachment of the ester group was thus unequivocally established to be at C-9. As in **6**, the ether bridge across the 10-membered ring from C-2 to C-8 was confirmed in a selective INEPT experiment wherein coupling between H-2 and C-8 was clearly observed. The relative stereochemistry of erythrolide F was the same as that in erythrolide E as shown by the NOE data in Table IV.

The ^1H NMR spectrum of compound **8**, erythrolide I, was very similar to that of **7** but contained only one acetate methyl signal and appeared not to have the signal for the methylene protons of the acetoxyacetate group. The signal at around δ 4.35, however, seemed broader and taller compared to the other signals in the spectrum. This signal integrated for three protons, and in the spectrum of a more concentrated sample of **8**, it was clear that there were two overlapped signals at this resonance. One of these was assigned as the signal for H-7 from its coupling with H-6 as indicated in the COSY spectrum. The other broad two-proton signal was shown by COSY to be coupled to a broad triplet signal at around δ 2.5. Upon addition of a few drops of CD_3OD, the latter signal disappeared and the broad singlet signal sharpened up. Since all the other signals had already been assigned from COSY to be those for protons on the ring system, the broad two-proton signal at δ 4.35 in the spectrum of **8** could only be that for the methylene protons of the C-9 ester group but, in this case, shifted by about 0.3 ppm upfield from its value in the spectrum of **7** and coupled with a hydroxyl proton. This information, along with the presence of a new carbonyl resonance in the ^{13}C NMR spectrum of **8** at δ 172.1 (replacing signals at δ 167.5 and 170.0 in **7**) as well as a slight shift in the methylene (from δ 60.5 in **7** to δ 61.1 in **8**) and C-9 (from δ 68.8 in **7** to δ 69.8 in **8**) resonances, was consistent with having a 9-α-hydroxyacetate in **8** instead of an α-acetoxyacetate group. This was supported in the mass spectrum by the occurrence of a peak at $M^+ - 75$ corresponding to cleavage of the C-9 carbon–oxygen bond.

Acetylation of **8** yielded a product identical by ^1H NMR with the acetylation product (**20**) of **7**, hence confirming that **8** is the 9-α-hydroxyacetate derivative of **7**. The relative stereochemistry of **8** was determined to be identical with that of **7** on the basis of NOE data (Table IV).

Compound **9**, erythrolide G, was isolated in trace amounts during purification of compound **6** by silica HPLC. The ^1H NMR spectrum of **9** differed from that of **6** in having a third acetate methyl signal. Also, it did not have the pair of mutually coupled downfield doublet signals nor a peak in the IR spectrum at around 1685 cm^{-1} characteristic of an α,β-unsaturated ketone. Compound **9** was instead found by ^1H spin decoupling data to have the three-proton allylic acetate spin system comprised by H-12 to H-14. The close similarity of the rest of the ^1H NMR spectrum of **9** with that of **6** led to the assignment of erythrolide G as the 12-acetoxy derivative of erythrolide E. Placement of the propenyl segment such that the double bond was at the 13,14-position (rather than at the alternative 12,13-position) was supported by the NOE observed between the Me-15 signal (δ 1.60) and the doublet signal at δ 5.77 (H-14) and the NOE between the Me-20 signal (δ 1.51) and the doublet at δ 5.71 (H-13). W-Coupling observed in the COSY spectrum between the Me-20

(20) Bax, A.; Feretti, J. A.; Nashed, N.; Jerina, D. *J. Org. Chem.* **1985**, *50*, 3029.

Table V. ^{1}H NMR Data for Compounds 10–13[a]

H at carbon	compound 10	11	12	13
2	5.16 [5.35, 1 H, d, 8.9][b]	5.17 (1 H)	5.27 [5.49, 1 H, d, 7.9][b]	5.25 (1 H9)
3	1.75 (1 H, m)	1.80 (1 H, m)	1.93 (1 H, m)	1.95 (1 H, m)
	1.62 (1 H, m)	1.67 (1 H, m)	1.70 (1 H, m)	1.70 (1 H, m)
4	2.57 (1 H, m)	2.60 (1 H, m)	2.42 (1 H, m)	2.42 (1 H, m)
	2.45 (1 H, m)	2.49 (1 H, m)	2.50 (1 H, m)	2.47 (1 H, m)
6	5.15 [5.46, 1 H, br d, 8.5][b]	5.18 (1 H)	5.24 [5.35, 1 H, d, 8.4][b]	5.25 (1 H)
7	5.15 [5.15, 1 H, d, 8.5][b]	5.18 (1)	5.24 [5.24, 1 H, d, 8.4][b]	5.25 (1 H)
9	5.81 (1 H, br s, 3.0)	5.86 (1 H, br s, 3.0)	5.72 (1 H, br, s, 4.0)	5.73 (1 H, d, 3.7)
10	2.20 (1 H, br s, 3.0)	2.23 (1 H, br s, 3.0)	2.87 (1 H, br s, 4.0)	2.87 (1 H, br s, 3.7)
12	3.51 (1 H, dt, 9.23, 3.2, 2.3)	3.56 (1 H, m)	2.92 (1 H, br s, 3.5)	2.93 (1 H, br s)
13	2.07 (1 H, ddd, 16.2, 3.7, 2.3)	2.12 (1 H, m)	2.18 (1 H, dd, 17.6, 2.2, 0.0)	2.16 (1 H, m)
	1.97 (1 H, ddd, 16.2, 3.2, 2.3)	2.03 (1 H, m)	2.08 (1 H, ddd, 17.6, 4.8, 3.5)	2.11 (1 H, m)
14	4.81 (1 H, br t, 3.7, 2.3)	4.91 (1 H, br t)	4.62 (1 H, dd, 4.8, 2.2)	4.91 (1 H, dd)
15	1.19 (3 H, s)	1.23 (3 H, s)	1.10 (3 H, s)	1.12 (3 H, s)
16	1.89 (3 H, s)	1.97 (3 H, br s)	1.88 (3 H, br s)	1.88 (3 H, br s)
18	1.74 (3 H, s)	1.80 (3 H, s)	1.65 (3 H, s)	1.67 (3 H, s)
20	1.12 (3 H, br s, 1.8)	1.16 (3 H, br s)	1.45 (3 H, br s)	1.45 (3 H, br s)
11-OH	3.10 (1 H, br s)	3.13 (1 H, br s)		
12-OH	2.91 (1 H, d, 9.23)	2.91 (1 H, d, 9.23)		
acetate	2.00 (3 H, s)	1.99 (3 H, s)	1.93 (3 H, s)	2.01 (3 H, s)
methyl	2.17 (3 H, s)	2.22 (3 H, s)	2.17 (3 H, s)	1.98 (3 H, s)
		2.06 (3 H, s)		1.98 (3 H, s)
butyrate	2.15 (2 H, t, 4.6)		2.24 (2 H, t)	
	1.56 (2 H, m, 4.6, 8.3)		1.61 (2 H, m)	
	0.90 (3 H, t, 8.3)		0.94 (3 H, t)	

[a] Spectra recorded in $CDCl_3$ at 300 MHz. Values reported in parts per million relative to internal TMS. [b] Bracketed data obtained in C_6D_6.

and H-10 signals indicated that these protons were trans to each other. Assuming a β-configuration for Me-20 as in compounds **2–8**, the allylic acetate group was consequently assigned the α configuration on the basis of the NOE between the Me-20 and H-12 signals. Other NOEs observed for **9** (Table IV) were similar to those observed in **6**.

Previously reported ether-cyclized briarein metabolites from gorgonians, e.g., pteroidine,[21] praeolide,[22] and juncellin A,[23] all have the ether bridge located between C-8 and C-4. The new erythrolides E, F, G, and I (**6–9**), which possess an unprecedented C-2 to C-8 ether link, thus comprise a new group of ether-cyclized briaranes.

Compound **5**, erythrolide H, differed from the compounds previously discussed in not having signals for an olefinic exocyclic methylene group in its ^{1}H NMR spectrum. However, the spectrum had an A,B quartet signal at δ 4.04, 3.95 which was coupled to an olefinic signal at δ 5.54 and could thus be reasonably assigned to the methylene protons of an allylic primary alcohol. The presence of this structural feature was supported by ^{13}C NMR resonances at δ 66.5 (t), 147.5 (s), and 118.3 (d). Its location in the structure of **5** was confirmed by decoupling and COSY data. The olefinic proton (δ 5.54) was allylically coupled to one of the C-4 methylene protons as well as to the signal at δ 5.20 (H-7). The rest of molecule was assumed to be the same as in compounds **3** and **4**, on the basis of NMR data (see Tables I and III).

NOE measurements (Table IV) for erythrolide H were consistent with a relative stereochemistry identical with that of erythrolide C (**3**). The large coupling constant of 10 Hz between the olefinic proton signal at δ 5.54 (H-6) and the methine proton at the lactone ring juncture (H-7, δ 5.20) suggested that these protons had an antiparallel orientation. The large NOE observed between the 8-OH proton and H-6 indicated that the olefin section of the 10-membered ring was folded downward relative to the β-oriented methyl group at C-1. Consequently, H-7 was assigned to be on the β face of the molecule.

Isolation and Structure Determination of New Briarane Derivatives from *Briareum* sp. The briareolides were isolated by standard methods as outlined in the Experimental Section.

Briareolide A (**10**) crystallized as colorless needles during slow evaporation of a SiO_2 flash chromatography fraction ($CHCl_3$–MeOH, 99:1) obtained from the dichloromethane extract. FAB$^+$ high-resolution mass spectrometry established a molecular formula for this compound of $C_{28}H_{40}O_{11}$ (found m/e 553.2674 $(M + H)^+$, calcd 553.2649), which was supported by ^{1}H (Table V) and ^{13}C NMR (Table VII) data. Absorptions in the infrared spectrum indicated the presence of hydroxyl (3460 cm^{-1}), γ-lactone (1775 cm^{-1}), and three other carbonyl groups (1760, 1730, and 1700 cm^{-1}). Resonances in the ^{13}C NMR spectrum of **10** at δ 172.6, 170.8, 169.8, and 168.3 supported the presence of a γ-lactone and three additional esters. Two of the esters were identified as acetates by the presence of methyl resonances in the ^{1}H NMR spectrum at δ 2.17 and 2.0. The other ester was determined to be a butyrate on the basis of the observation in the ^{1}H NMR spectrum of signals for a propyl group: a two-proton triplet at 2.15 ppm, a two-proton multiplet at 1.56 ppm, and a methyl triplet at 0.9 ppm. Further evidence for the presence of a butyrate ester in **10** was provided by its low-resolution EI$^+$ mass spectrum, where fragment ions corresponding to losses of a butyroxy group (m/e 465.2) and butyric acid (m/e 464.2) were observed. Two CD_3OD-exchangeable protons [δ 3.10 (1 H, br s) and 2.91 (1 H, d, J = 9.23 Hz)] observed in the ^{1}H NMR spectrum suggested the presence of two hydroxyl groups. Ten of the 11 oxygen atoms in the molecular formula of compound **10** were accounted for by the γ-lactone, ester, and hydroxyl groups. Because all the hydrogens had already been accounted for (by a ^{13}C DEPT experiment), the remaining oxygen was assigned as a fully

(21) Clastres, A.; Ahond, A.; Poupat, C.; Potier, P.; Kan, S. K. *J. Nat. Prod.* **1984**, *47*, 155.
(22) Luo, Y.; Long, K.; Fang, Z. *Zhongshan Daxue Xuebao, Ziran Kexueban*, **1983**, *No. 1*, 83; *Chem. Abstr.* **1983**, *99*, 50572c.
(23) Yao, J.; Qian, J.; Fan, H.; Shih, K.; Huang, S.; Lin, Y.; Long, K. *Chem. Abstr.* **1984**, *101*, 211491.

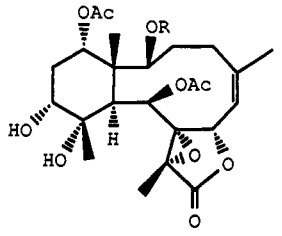

10 Briareolide A, R = (CO)Pr

11 Briareolide B, R = Ac

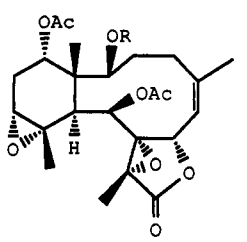

12 Briareolide C, R = (CO)Pr

13 Briareolide D, R = Ac

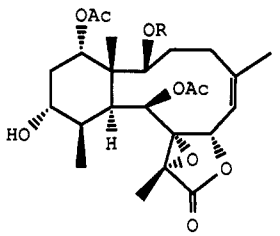

14 Briareolide E, R = (CO)Pr

15 Briareolide F, R = Ac

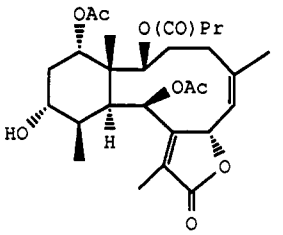

16 Briareolide G

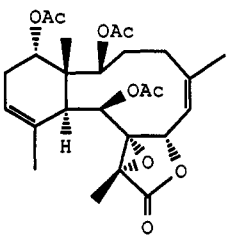

17 Briareolide H

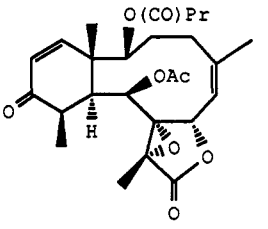

18 Briareolide I

substituted epoxide on the basis of ^{13}C NMR evidence [resonances at δ 66.0 (s) and 70.6 (s)]. Olefinic resonances in the ^{13}C NMR spectrum at δ 143.6 (s) and 118.0 (d) indicated the presence of a trisubstituted double bond. The three ester groups, γ-lactone, carbon–carbon double bond, and epoxide functionalities accounted for seven of the nine double-bond equivalents required by the molecular formula. Compound **10**, therefore, contained two other rings in its structure aside from the lactone and epoxide.

Analysis of the data from ^1H NMR double resonance decoupling and COSY experiments led to the elucidation of the three parts of the molecular framework of **10** shown in Figure 4. The ^1H and ^{13}C chemical shift assignments are based on data from a ^1H–^{13}C correlation experiment (HETCOR, J = 140 Hz). The location of each of the ester groups was assigned definitively from evidence provided by long-range HETCOR and selective INEPT experiments. The resonances at δ 169.8 and 168.3 were assigned as acetate carbonyls by their coupling with the acetate methyl ^1H signals at δ 2.0 and 2.17, respectively (long-range HETCOR, J = 10 Hz); the resonance at δ 170.8 was assigned as the lactone carbonyl due to a correlation with the secondary methyl signal at δ 1.74; finally, the signal at δ 172.6 was coupled with the methylene signal at δ 2.15 and was consequently assigned as the butyrate carbonyl. Through INAPT experiments (J = 6 Hz) it was possible to correlate each ester carbonyl carbon with its neighboring methine proton. The connectivities between each structural unit were then deduced from observation of two- and three-bond ^1H–^{13}C couplings in a long-range HETCOR experiment (see Table X). Placement of the epoxide at the α,β-position of the γ-lactone was deduced from the

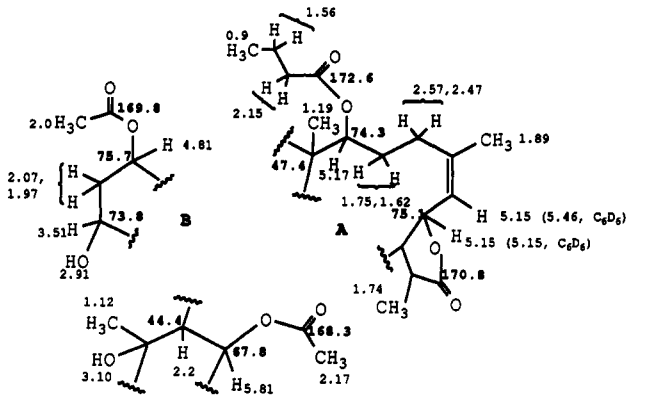

Figure 4. Partial structures and NMR assignments for briareolide A (**10**).

coupling observed between the quaternary methyl protons at δ 1.74 (methyl group α to the carbonyl) and the epoxide carbons at δ 70.6 and 66.0. Key H/C correlations for confirming the skeleton in the lactone region of **10** were those observed between the methine proton at δ 5.81 (H-9) and both the epoxide carbons (δ 70.6 and 66.0), as well as with the methine carbon at δ 75.1. The relative chemical shift assignment of the epoxide carbons was confirmed by a correlation observed in an INAPT experiment between the ring juncture methine proton (H-10, δ 2.20) and the carbon at δ 70.6 (C-8).

Much of the relative stereochemistry of compound **10** was determined by NOE difference spectroscopy, the results of which are shown in Table IX. Irradiation of the ring juncture methyl at C-15 (δ 1.19) resulted in enhancement of the acetoxy methine proton at C-14 (δ 4.81), which was also enhanced upon irradiation of the methyl at δ 1.12 (Me-20). A large NOE enhancement was also observed for the methine proton at C-12 (δ 3.51) when Me-20 was irradiated. Hence, protons resonating at δ 1.19, 4.81, 1.12, and 3.51 were all on the same side of the molecule arbitrarily assigned as the β face. The C-11 hydroxyl proton at δ 3.10, C-10 methine proton (δ 2.20), butyroxy methine (δ 5.14) at C-2, and acetoxy methine (δ 5.81) at C-9 were all found to be within NOE proximity on the other (α) face of the molecule on the basis of the NOE data given in Table IX. A large coupling between the vinyl proton at C-6 and the methine proton at C-7 suggested an antiparallel orientation of these protons; thus H-7 and H-6 must be directed toward opposite faces of the molecule. There were no NOE data, however, to establish the configuration at either one of these carbons. This left the stereochemistry at C-7 as well as that at the C-8,C-17 epoxide unassigned at this point. A large NOE enhancement of the acetoxy methine proton at C-9 (δ 5.81) was observed upon irradiation of the signal (δ 1.74) for the methyl group on the lactone ring. However, this evidence was not sufficient to assign the stereochemistry of the epoxide since examination of Dreiding molecular models showed that this NOE enhancement would be equally likely observed in both α- and β-epoxide isomers.

The stereochemistry of **10** was fully defined by analogy with compound **11** (briareolide B), another major crystalline metabolite isolated from a slightly more polar fraction of the same extract. This compound showed infrared absorptions similar to those of compound **10** that clearly indicated the presence of hydroxyl, ester, and γ-lactone functionalities. The ^1H and ^{13}C NMR spectra of **11** were nearly identical with those of **10** except for the following differences: the signals for the propyl group of the butyrate ester were missing in the ^1H NMR spectrum

Table VI. ^{1}H NMR Data for Compounds 14–18[a]

H at carbon	compound 14	15	16[b]	17	18
2	5.15 (1 H, d, 7.5)	5.12 (1 H, d, 7.5)	5.05 (1 H, d, 5.6)	5.03 (1 H, d, 6.3)	5.01 (1 H, d)
3	1.68 (1 H, dd, 13.2, 7.5)	1.70 (1 H, m)	1.79 (2 H, m)	1.72 (2 H, m)	2.40 (1 H, m)
	1.95 (1 H, dd, 13.2, 3.5)	1.95 (1 H, m)			2.57 (1 H, m)
4	2.52 (1 H, m)	2.53 (1 H, m)	1.98 (1 H, m)	2.55 (2 H, m)	1.95 (1 H, m)
	2.63 (1 H, m)	2.62 (1 H, m)	1.78 (1 H, m)		1.90 (1 H, m)
6	5.34 (1 H, d, 9.3)	5.24 (1 H, d, 9.4)	5.29 (1 H, d, 7.9)	5.42 (1 H, d, 9.3)	5.35 (1 H, br d, 9.6)
7	5.29 (1 H, d, 9.3)	5.29 (1 H, d, 9.4)	5.20 (1 H, br)	5.36 (1 H, d, 9.3)	5.60 (1 H, d, 9.6)
9	5.56 (1 H, d, 2.2)	5.56 (1 H)	6.42 (1 H, br s)	5.69 (1 H, d, 3.0)	5.37 (1 H, d, 3.5)
10	2.20 (1 H, dd, 4.4, 2.2)	2.20 (1 H, m)	2.19 (1 H, m)	2.83 (1 H, m)	2.80 (1 H, dd, 11.0, 3.5)
11	1.98 (1 H, dd, 6.6, 4.4)	1.98 (1 H, m)	1.98 (1 H, m)	–	2.57 (1 H, dd, 11.0, 6.9)
12	3.72 (1 H, ddd, 10.5, 4.4, 2.2)	3.70 (1 H, m)	3.86 (1 H, br s)	5.42 (1 H, m)	–
13	1.73 (1 H, ddd, 15.4, 4.4, 2.2)	1.75 (1 H, ddd, 15.4, 4.4, 2.2)	2.03 (2 H, m)	2.22 (1 H, m)	5.95 (1 H, d, 10.5)
	2.03 (1 H, ddd, 15.4, 2.6, 2.2)	2.02 (1 H, ddd, 15.4, 2.6, 2.2)		2.04 (1 H, m)	6.31 (1 H, d, 10.5)
14	4.86 (1 H, br t, 2.2, 2.6)	4.89 (1 H, br t)	4.95 (1 H, br t)	4.74 (1 H, br t, 3.3)	
15	1.02 (3 H, s)	1.02 (3 H, s)	1.13 (3 H, s)	1.02 (3 H, s)	1.12 (3 H, s)
16	2.03 (3 H, s)	2.02 (3 H, s)	1.82 (3 H, br s)	2.03 (3 H, s)	1.82 (3 H, br s)
18	1.62 (3 H, s)	1.62 (3 H, s)	2.21 (3 H, br s)	1.56 (3 H, s)	1.53 (3 H, s)
20	1.26 (3 H, d, 6.6)	1.26 (3 H, d, 6.6)	1.14 (3 H, d, 6.9)	1.84 (3 H, br s)	1.33 (3 H, d, 6.9)
12-OH	2.11 (1 H, d, 10.5)	2.12 (1 H, d, 10.5)	–	–	–
acetate	2.19 (3 H, s)	2.19 (3 H, s)	2.10 (3 H, s)	2.16 (3 H, s)	2.16 (3 H, s)
methyl	2.03 (3 H, s)	2.03 (3 H, s)	1.99 (3 H, s)	2.04 (3 H, s)	
		2.00 (3 H, s)		1.95 (3 H, s)	
butyrate	2.24 (2 H, t)		2.19 (2 H, t, 7.6)		2.46 (2 H, t, 7.5)
	1.60 (2 H, m)		1.59 (2 H, m)		1.75 (2 H, m)
	0.95 (3 H, t, 7.2)		0.93 (3 H, t)		1.02 (3 H, t, 6.9)

[a] Spectra recorded in $CDCl_3$ at 300 MHz; values in parts per million relative to TMS. [b] Spectrum recorded at 60 °C.

Table VII. ^{13}C NMR Data for Compounds 10–13[a]

carbon	compound 10[b]	11	12[b]	13
1	47.4 (s)	47.4 (s)	44.4 (s)	44.4 (s)
2	74.3 (d)	74.7 (d)	73.0 (d)	73.5 (d)
3	31.9 (t)	31.4 (t)	31.1 (t)	31.0 (t)
4	28.2 (t)	28.2 (t)	28.2 (t)	28.2 (t)
5	143.6 (s)	143.6 (s)	144.5 (s)	144.6 (s)
6	118.9 (d)	118.9 (d)	118.6 (d)	118.6 (d)
7	75.1 (d)	75.0 (d)	75.3 (d)	75.3 (d)
8	70.6 (s)	70.6 (s)	69.9 (s)	69.9 (s)
9	67.8 (d)	67.8 (d)	69.6 (d)	69.7 (d)
10	44.4 (d)	44.5 (d)	42.3 (d)	42.8 (d)
11	74.6 (s)	74.7 (s)	59.2 (s)	59.2 (s)
12	73.4 (d)	73.9 (d)	58.7 (d)	58.6 (d)
13	27.5 (t)	27.6 (t)	25.9 (t)	26.0 (t)
14	75.7 (d)	75.8 (d)	72.1 (d)	72.1 (d)
15	14.5 (q)	14.5 (q)	15.0 (q)	15.1 (q)
16	27.2 (q)	27.2 (q)	26.9 (q)	26.8 (q)
17	66.0 (s)	66.1 (s)	64.5 (s)	64.4 (s)
18	10.4 (q)	10.5 (q)	10.6 (q)	10.7 (q)
19	170.8 (s)	170.7 (s)	170.5 (s)	170.5 (s)
20	22.6 (q)	22.5 (q)	24.2 (q)	24.2 (q)
acetate	168.3 (s)	168.2 (s)	169.2 (s)	169.2 (s)
	21.3 (q)	21.3 (q)	21.1 (q)	21.3 (q)
	169.8 (s)	169.8 (s)	170.9 (s)	170.9 (s)
	21.7 (q)	21.7 (q)	21.3 (q)	21.1 (q)
		170.2 (s)		169.8 (s)
		21.3 (q)		21.1 (q)
butyrate	172.6 (s)		172.3 (s)	
	36.3 (t)		36.2 (t)	
	18.1 (t)		18.2 (t)	
	13.7 (q)		13.7 (q)	

[a] Spectra recorded in $CDCl_3$ at 75 MHz; values in parts per million relative to TMS. Multiplicities from DEPT experiment unless otherwise specified. [b] Assignments from HETCOR experiment (J = 140 Hz).

of compound **11**, and an additional acetate signal at δ 2.06 was observed; likewise, ^{13}C signals for the butyrate group were replaced by resonances associated with an acetate group [δ 170.2 (s) and 21.3 (q)]; the C-2 carbon in **11** had a chemical shift of 74.7 ppm, which is downfield by 0.4 ppm from the value in compound **10** (see Table VII); lastly, the carbonyl carbon of the acetate group at C-2 of compound **11** had a chemical shift of δ 170.2, 2.4 ppm upfield of the value in compound **10**. On these grounds, **11** was determined to be the 2-acetoxy analogue of **10**. X-ray crystallographic analysis of **11** confirmed this conclusion, established the stereochemistry at the epoxide and lactone junctures, and determined the absolute configuration to be that shown in the drawing (see X-ray discussion below.)

Thus the stereochemical assignments made on the basis of NOE data were proven to be correct. Since the ^{1}H and ^{13}C NMR spectra of compound **10** and compound **11** were virtually identical, and similar NOEs were observed in both compounds, it was concluded that these compounds have the same stereochemistry at all of the ring junctures and chiral centers in their structures, including that at the epoxide. This stereochemistry compared favorably with that of other briarein-type compounds reported in the literature.

Compound **12** (briareolide C) shared many spectral features in common with compound **10**. Its infrared spectrum indicated the presence of γ-lactone (1780 cm^{-1}) and ester (1760 and 1730 cm^{-1}) functionalities, but contained no absorption for a hydroxyl group. A molecular formula of $C_{28}H_{38}O_{10}$ established for this compound by high-resolution FAB^+ mass spectrometry was supported by ^{1}H and ^{13}C NMR data (Tables V and VII). The ^{1}H NMR spectrum of **12** lacked the C-11 and C-12 CD_3OD-exchangeable OH proton signals observed in the spectrum of **10**. Other noticeable differences were downfield shifts of H-10 (from δ 2.20 in compound **10** to δ 2.87 in compound **12**), H-2 (from δ 5.14 to 5.27), and Me-20 (from δ 1.12 to 1.45). Careful examination of the ^{13}C NMR spectrum of **12** in comparison with that of **10** revealed that there were considerable differences in chemical shifts of the carbons in the six-membered ring, i.e., C-10 to C-14 and C-1, as well as in carbons 2, 9, and 20. The difference was most discernible at carbons 11 and 12 (δ 59.2 and 58.7 in **12** vs δ 74.6 and 73.4 in **10**). These NMR data for **12** were consistent with its having an epoxide at the 11,12-position in lieu of the diol functionality found in **10**. The remainder of the ^{13}C NMR spectrum of **12** was virtually superim-

Table VIII. ^{13}C NMR Data for Compounds 14–18[a]

carbon	compound 14[b]	15	16[c]	17[c]	18[c]
1	46.1 (s)	46.1 (s)	46.3 (s)	46.0 (s)	45.0 (s)
2	74.6 (d)	75.9 (d)	75.7 (d)	74.9 (d)[d]	74.4 (d)[d]
3	32.3 (t)	32.2 (t)	32.2 (t)	28.6 (t)	28.2 (t)
4	28.7 (t)	28.7 (t)	32.2 (t)	27.0 (t)	27.1 (t)
5	145.8 (s)	145.8 (s)	154.2 (s)[e]	146.2 (s)	144.6 (s)
6	117.8 (d)	117.9 (d)	114.1 (d)	118.2 (d)	119.7 (d)
7	75.1 (d)	75.1 (d)	72.2 (d)	74.5 (d)[d]	71.3 (d)[d]
8	70.3 (s)	70.3 (s)	161.6 (s)[e]	70.7 (s)	63.9 (s)
9	69.5 (d)	69.4 (d)	78.4 (d)	68.8 (d)	69.6 (d)
10	41.1 (d)	41.1 (d)	33.9 (d)	43.6 (d)	43.6 (d)
11	38.5 (d)	38.5 (d)	38.7 (d)	133.5 (d)	43.5 (d)
12	71.3 (d)	71.2 (d)	71.4 (d)	120.8 (d)	198.8 (s)
13	30.4 (t)	30.4 (t)	30.5 (t)	32.5 (t)	125.6 (d)
14	76.5 (d)	76.5 (d)	76.8 (d)	73.5 (d)[d]	153.8 (d)
15	14.3 (q)	14.2 (q)	14.3 (q)[e]	15.1 (q)	15.5 (q)
16	27.0 (q)	26.9 (q)	25.4 (q)[e]	26.3 (q)	25.1 (q)
17	63.9 (s)	63.9 (s)	124.1 (s)[e]	63.3 (s)	62.5 (s)
18	9.81 (q)	9.81 (q)	11.9 (q)[e]	9.80 (q)	9.90 (q)
19	170.8 (s)	170.9 (s)	173.4 (s)	170.5 (s)	169.9 (s)
20	19.7 (q)	19.7 (q)	17.5 (q)	24.4 (q)	17.5 (q)
acetate	169.3 (s)	169.3 (s)	169.5 (s)	170.5 (s)	169.9 (s)
	21.4 (q)	21.3 (q)	21.2 (q)	21.4 (q)	21.4 (q)
	169.9 (s)	170.0 (s)	169.7 (s)	168.9 (s)	
	21.6 (q)	21.4 (q)	20.9 (q)	21.3 (q)	
		170.5 (s)		171.1 (s)	
		21.6 (q)		21.2 (q)	
butyrate	172.9 (s)		172.6 (s)		172.4 (s)
	36.4 (t)		36.2 (t)		36.3 (t)
	18.2 (t)		18.2 (t)		18.4 (t)
	13.7 (q)		13.6 (q)		13.8 (q)

[a] Spectra recorded in $CDCl_3$ at 75 MHz; values in parts per million relative to TMS. Multiplicities from DEPT experiment unless otherwise specified. [b] Assignments from HETCOR experiment (J = 140 Hz). [c] Multiplicities obtained by APT; assignments by analogy. [d] Signals within a column may be interchanged. [e] Broad signal.

Table IX. NOE Data for Briareolides A, B, C, E, G, and I

irr signal	enhanced signal (%) 10	11	12	14	16	18
H-2	H-10 (10.5)		H-10 (10.7)		H-10 (3)	H-14
Me-15	H-14 (2.3)	H-14 (9.8)	H-14 (10), H-2 (2)	H-14 (15.3)	H-14 (9.5)	H-14 (10.2)
Me-16	H-6 (4.5)	H-6 (7.5)		H-6		
Me-18	H-9 (18.8)	H-9 (15)		H-9 (8.4)		H-9
Me-20	H-9 (15.8), H-12 (12.3), H-14 (2.6)	H-9 (11.9), H-12	H-9 (15), H-12 (10.6)	H-9 (13.3), H-12 (6.8)	H-12 (7)	H-9 (6.4)
11-OH	H-10 (8)	H-10 (6.4), H-9 (4)				
H-6					Me-16	
H-9			H-10 (6), Me-20 (2.7), Me-18 (2.7)		H-10 (2), Me-20 (4)	
H-10				H-2 (4.4)		H-9
H-14						H-15 (3)

Table X. Long-Range H/C Correlations in Compounds 10, 12, and 14

10		12		14	
H	C	H	C	H	C
H-9	C-7, C-8, C-17	H-9	C-7, C-8, C-1, C-10, C-11	H-9	C-7, C-8, C-10
H-10	C-1, C-8			H-2	C-1, C-14, C-4
H-14	C-1, C-10	H-10	C-8	H-14	C-12
Me-15	C-1	H-14	C-1, C-10		
Me-18	C-17, C-8	H-7	C-19		
Me-20	C-12	Me-20	C-10		

posable with that of 10 (see Table VII). Consequently, it was assumed that the rest of the structure of 12 was the same as in 10. This was confirmed by ^1H–^{13}C correlations from HETCOR and selective INEPT experiments (see Table X).

The relative stereochemistry of 12, determined by NOE difference spectroscopy, was also found to be identical with that of 10. An NOE interaction that was not seen in compound 10, but was detected in 12, was that between the proton at C-2 and the vinyl methyl group (Me-16). This suggested that the section of the 10-membered ring bearing the double bond was folded downward relative to the axial (β) ring juncture methyl. Assignment of H-7 as being β-oriented readily followed from this since the large coupling constant between H-7 and H-6 (8.4 Hz observed in C_6D_6) indicated that these two protons were antiparallel to each other. The 11,12-epoxide in 12 was assigned as α on the basis of the observed NOE enhancement of H-9 but not of H-10 upon irradiation of the Me-20 signal. If the epoxide were β, an NOE interaction would have been expected between H-10 and Me-20 on the basis of examination of a Dreiding model representing such stereochemistry. The observation of this NOE interaction has in fact been reported[12] for briaranes containing an 11β,12β-epoxide. To date, only the 11,12-epoxide β isomer has been found in gorgonians.[10,12] The only known 11α,12α-epoxy-containing briarane diterpenes, stylatulide[15] and 17-*epi*-stylatulide,[24] were isolated from a sea pen, *Stylatula*

sp. Briareolide C (12) is thus the first reported 11α,12α-epoxy briarane from a gorgonian.

Compound 13 (briareolide D) was easily identified as the 2-acetoxy analogue of 12 from comparison of their ^1H and ^{13}C NMR spectra. The ^1H NMR spectrum of 13 contained three (vs two in 12) acetate methyl signals and lacked the characteristic signals for the propyl group of a butyrate ester. Corresponding differences in the ^{13}C NMR spectra of 13 and 12 were observed that further supported the structure of 13 (see Table VII).

High-resolution mass spectrometry established a molecular formula of $C_{28}H_{40}O_{10}$ for briareolide E, compound 14. Observation in the infrared spectrum of absorptions at 3560, 1782, 1740, and 1732 cm^{-1} suggested that this compound possessed the same functional groups as in compounds 10–13, i.e., hydroxyl, γ-lactone, and ester carbonyls. The difference in structure between 14 and 10 was evident from comparison of their ^1H and ^{13}C NMR spectra. The ^1H NMR spectrum of 14 contained a doublet methyl signal (δ 1.26, J = 6.6) and only one hydroxyl proton signal (δ 2.11, J = 10.5, exchangeable by addition of CD_3OD). There was an additional methine carbon signal (δ 38.5), but there were one fewer oxygenated carbon signals in the spectrum of 14 when compared to the spectrum of 10. ^1H NMR homodecoupling and COSY experiments established the extended spin system from H-9 to H-14 with a branching methyl at C-11. The rest of the molecular framework of 14 was assigned to be the same as in compound 10 on the basis of correspondence of ^1H and ^{13}C NMR data (see Tables VI and VIII) and confirmatory evidence provided by HETCOR and selective INEPT experiments (Table X). Compound 14 was therefore the 11-deoxy analogue of compound 10. The relative stereochemistry of 14 was determined by NOE measurements and was shown (Table IX) to be the same as that of the previously described briareolides.

Compound 15 (briareolide F) was easily identified as the C-2-acetoxy derivative of 14 on the basis of the absence of signals for the propyl group and the presence of an additional acetate methyl signal at δ 1.99 in the ^1H NMR spectrum of 15. This was further supported by ^{13}C NMR data. The signals for the butyrate group in the ^{13}C NMR spectrum of 14 were replaced in the spectrum of 15 by resonances for an acetyl group [δ 170.5 (s) and 21.6 (q)], and the chemical shift of C-2 in 15 (δ 75.0) was 0.4 ppm lower than in 14. The rest of the signals in the ^1H and ^{13}C NMR spectra of 15 were virtually identical with those in 14 (see Tables VI and VIII).

Compound 17 (briareolide H), isolated as a white powder, was a minor component of the least polar of the diterpene-containing fractions from this organism. Except for not having an absorption for a hydroxyl group, the infrared spectrum of 17 was very similar to that of 15, suggesting the close structural similarity of these two compounds. The difference in their structures was revealed by comparison of their ^{13}C NMR spectra. Whereas 15 had only two olefinic resonances in its ^{13}C NMR spectrum [δ 145.8 (s) and 117.9 (d)], that of 17 contained four [δ 146.2 (s), 133.5 (s), 120.8 (d), and 118.2 (d)], confirming the presence in 17 of an additional trisubstituted double bond. Moreover, there was one fewer oxygenated carbon signal in the spectrum of 17. The molecular weight of 17 was 18 mass units less than that of 15, i.e., the molecular formula of 17 differed from that of 15 by a molecule of H_2O. These IR, MS, and ^{13}C NMR data pointed to 17 as conceivably being a dehydration product of the alcohol 15.

The ^1H NMR spectrum of 17 contained two overlapping olefinic signals at δ 5.42, one of which was assigned as H-6 from its couplings (observed by COSY) with the allylic methylene proton signals (C-4) and the vinylic methyl group at δ 2.03. Observation in the ^1H and ^{13}C NMR spectra of 17 of signals closely matching in chemical shifts those for all positions in the 10-membered ring and the epoxy–lactone moiety of 15 (see Tables VI and VIII) strongly supported the assumption that this part of the molecule was identical in the two compounds. Coupling from H-2 through to H-7 and between H-9 and H-10 was confirmed from the COSY plot.

The other olefinic proton signal at δ 5.42 was shown by COSY to be long-range coupled to the methyl resonance at δ 1.84 (H-20) as well as to the multiplet at δ 2.04 (H-13), which was in turn coupled to the triplet at δ 4.74 (H-14). These data supported the six-membered-ring structure of 17. Spectral evidence for fusing the six- and 10-membered rings consisted of W-coupling between H-10 (δ 2.83) and Me-20 (δ 1.84) observed in the COSY spectrum and a NOE observed between the ring juncture methyl (Me-15, δ 1.02) and the acetoxy methine proton at δ 4.74 (H-14).

The relative stereochemistry of 17 was assigned on the basis of analogy with the previously described briareolides and was in part supported by NOE data (Table IX).

Compound 18 (briareolide I), $C_{26}H_{34}O_8$ by high-resolution mass spectral analysis, was isolated from the same fraction as compound 17. The infrared spectrum of 18 featured absorptions that indicated the presence of three different carbonyl types: γ-lactone (1782 cm^{-1}), ester (1735 cm^{-1}), and α,β-unsaturated ketone (1682 cm^{-1}). The latter structural feature, not found in the other briarane diterpenes in this series, was further supported by a UV absorption maximum at 217 nm (MeOH, ε 5614), the presence of signals at δ 198.8 (s), 125.6 (d), and 153.8 (d) in the ^{13}C NMR spectrum, and the presence of a mutually coupled pair of doublet signals (J = 10.5 Hz) in the ^1H NMR spectrum at δ 5.95 and 6.31 corresponding to the α and β olefinic protons, respectively. Another feature of the ^1H NMR spectrum of 18 was a methyl doublet signal at δ 1.33 that was coupled to a signal which from its chemical shift of 2.57 ppm could be assigned to the proton α to a carbonyl group. This latter signal was in turn coupled to a signal at δ 2.80, assigned as H-10 by its coupling with H-9 (δ 5.37). The NMR data presented thus far were accommodated by the partial structure shown below.

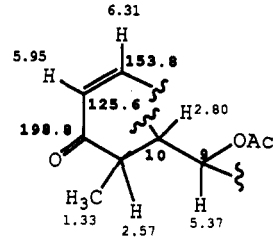

The rest of the ^1H and ^{13}C NMR data accounted for partial structures similar to those in the briareolides discussed earlier (see Tables V–VIII for pertinent data). An NOE enhancement of the doublet signal at δ 6.31 upon irradiation of the ring juncture methyl at δ 1.12 and also upon irradiation of the signal at δ 5.05 (H-2) confirmed the placement of the enone function in the six-membered ring as shown in the structure of 18.

Other NOE data for 18 are given in Table IX and support the relative stereochemistry at some of the chiral

(24) Faulkner, D. J.; Wratten, S. J. *Tetrahedron* **1979**, *35*, 1907.

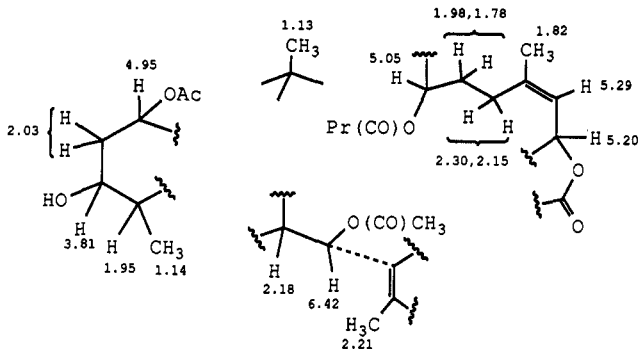

Figure 5. Partial structures for briareolide G (16).

centers. The rest of the stereochemical assignments for 18 were based on analogy with the other briareolides.

Compound 16 (briareolide G) was isolated as a white powder after purification by reversed-phase HPLC (MeOH–H_2O, 85:15) and was the most polar of the compounds reported in this series. Absence in the infrared spectrum of 16 of a peak at ~1775 cm^{-1} suggested that this compound did not possess the saturated γ-lactone functionality present in the structure of compounds 10–15, 17, and 18. There was, however, a carbonyl absorption in the IR spectrum at 1748 cm^{-1} which was characteristic of the carbonyl stretching of an α,β-unsaturated γ-lactone. The presence of this functionality was supported by a UV absorption at λ_{max}(MeOH) 204 (ε 9020). Other peaks in the IR spectrum of 16 at 3530 (OH) and 1736 (ester carbonyl) cm^{-1} suggested that, aside from the difference pointed out in the γ-lactone functionality, compound 16 had structural features similar to those of the previously described briareolides.

A molecular formula of $C_{28}H_{40}O_9$ was inferred for 16 from the FAB^+ mass spectrum. Peaks for fragment ions corresponding to losses of 1 molecule of butyric acid, 2 units of acetic acid, and 1 molecule of H_2O were observed, suggesting the presence of substituents similar to those in compound 14.

The ^1H NMR spectrum of 16 in $CDCl_3$ at normal temperature (~20 °C) contained a number of broadened signals. In the spectrum obtained at 60 °C, some of the broad signals were resolved and sharpened. Although many of the upfield signals were overlapped, analysis of the COSY spectrum and analogy with 14 allowed elucidation of the partial structures shown in the figure below.

The most downfield signal (δ 6.42) was assigned as H-9 since it was coupled with only one other signal (H-10, δ 2.18), and its chemical shift, much lower than that observed in the briareolides in this series (see Tables V and VI), could be accounted for by its being allylic as well as ester-bearing. Piecing together the structural units in Figure 5 based on NOE data (see Table IX) and analogy with the other briareolides resulted in the gross structure below proposed for compound 16.

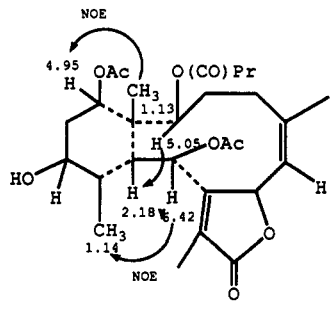

Coupling and NOE data (Table IX) supported the stereochemical assignments for 16. The only unassigned stereochemistry was that at C-7. However, H-7 could be assumed to be β, just as in the other briareolides, since the stereochemistry at all the other stereocenters in 16 was shown to be identical with that of the other compounds in this series.

Table XI. Atomic Parameters[a]

atom	x	y	z	U(eq)[b]
O-1	0.2926 (1)	0.55000	0.2573 (2)	0.0285 (5)
O-2	0.4485 (1)	0.5319 (2)	0.4363 (2)	0.0409 (6)
O-3	0.1102 (1)	0.1181 (2)	0.5948 (1)	0.0248 (4)
O-4	0.0958 (1)	−0.0914 (2)	0.6272 (1)	0.0301 (4)
O-5	0.2516 (1)	0.0421 (2)	0.4400 (1)	0.0233 (4)
O-6	0.0182 (1)	0.2208 (2)	0.1864 (1)	0.0191 (4)
O-7	−0.0787 (1)	0.0671 (2)	0.2542 (1)	0.0277 (4)
O-8	0.2227 (1)	−0.0173 (2)	0.0982 (1)	0.0287 (5)
O-9	0.4079 (1)	0.0859 (2)	0.0841 (2)	0.0346 (5)
O-10	0.4223 (1)	0.3297 (2)	0.2071 (1)	0.0235 (4)
O-11	0.5315 (2)	0.4503 (3)	0.1222 (2)	0.0569 (7)
C-1	0.2227 (1)	0.3472 (2)	0.1478 (2)	0.0190 (5)
C-2	0.2494 (1)	0.4251 (2)	0.2828 (2)	0.0193 (5)
C-3	0.1505 (1)	0.4572 (2)	0.3334 (2)	0.0202 (5)
C-4	0.1859 (2)	0.4990 (2)	0.4833 (2)	0.0234 (5)
C-5	0.2569 (1)	0.4032 (2)	0.5817 (2)	0.0216 (5)
C-6	0.2371 (1)	0.2779 (2)	0.5793 (2)	0.0212 (5)
C-7	0.1356 (1)	0.2059 (2)	0.4960 (2)	0.0197 (5)
C-8	0.1521 (1)	0.1173 (2)	0.3849 (2)	0.0179 (5)
C-9	0.1198 (1)	0.1461 (2)	0.2320 (2)	0.0174 (5)
C-10	0.2128 (1)	0.2003 (2)	0.1750 (2)	0.0169 (5)
C-11	0.2107 (1)	0.1125 (2)	0.0499 (2)	0.0219 (5)
C-12	0.3081 (2)	0.1392 (2)	−0.0070 (2)	0.0263 (6)
C-13	0.3218 (2)	0.2809 (3)	−0.0286 (2)	0.0274 (6)
C-14	0.3246 (2)	0.3629 (2)	0.0938 (2)	0.0232 (6)
C-15	0.1231 (2)	0.4090 (2)	0.0411 (2)	0.0250 (5)
C-16	0.3909 (2)	0.5917 (3)	0.3415 (2)	0.0346 (7)
C-17	0.4167 (3)	0.7226 (4)	0.2996 (4)	0.061 (1)
C-18	0.3566 (2)	0.4588 (3)	0.6876 (2)	0.0281 (6)
C-19	0.1438 (1)	−0.0155 (2)	0.4296 (2)	0.0217 (5)
C-20	0.1162 (1)	−0.0051 (2)	0.5611 (2)	0.0222 (5)
C-21	0.1120 (2)	−0.1350 (2)	0.3477 (2)	0.0308 (7)
C-22	−0.0775 (1)	0.1639 (2)	0.1924 (2)	0.0196 (5)
C-23	−0.1776 (2)	0.2361 (2)	0.1100 (2)	0.0262 (6)
C-24	0.1014 (2)	0.1167 (3)	−0.0669 (2)	0.0269 (6)
C-25	0.5200 (2)	0.3774 (3)	0.2084 (2)	0.0325 (7)
C-26	0.6114 (2)	0.3333 (3)	0.3298 (3)	0.0403 (8)

[a] Estimated standard deviations are within parentheses. [b] $U(eq) = {}^1/_3\sum_i\sum_j U_{ij}a_i^*a_j^*(\mathbf{a}_i\cdot\mathbf{a}_j)$.

Briareolide B (11): X-ray Crystal Structure. The final atomic parameters of the non-hydrogen atoms are listed in Table XI. A stereo ORTEP[25] drawing of a single molecule of briareolide B (11) is shown in Figure 6. The X-ray structure demonstrates the presence of a novel structural feature, that of an α,β-epoxy γ-lactone instead of a more commonly observed β-hydroxy-α-methyl γ-lactone, found in briarein A,[1] or an unsaturated α-methyl γ-lactone, seen in brianthein W.[9] The absolute configuration determined in the X-ray diffraction experiment is shown in the figure and is the same as found in other briareins and briantheins.

Bond distances and angles are generally within the range of observed geometries of related compounds. The ring C–C bonds involving the two bridging carbon atoms are all longer than a normal C–C single bond length and range between 1.556 (2) and 1.577 (2) Å. The conformation of the 10-membered ring is closely similar to those found in brianthein W and two new briareins reported by Bowden and co-workers.[12] Briareolide B forms one intramolecular hydrogen bond, O(8)–H···O(9) with O(8)···O(9) = 2.616 (2) Å, O(9)···H = 2.03 (3) Å, and angle O(8)–H···O(9) = 125

(25) Johnson, C. K. ORTEP II. Report ORNL-3794, revised; Oak Ridge National Laboratory: Oak Ridge, TN 1976.

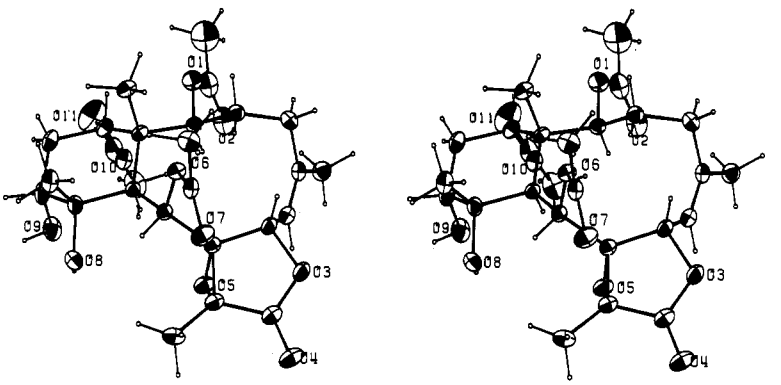

Figure 6. A stereo ORTEP plot of briareolide B (11) showing absolute configuration.

(2)°, and one intermolecular O–H···O hydrogen bond, O(9)–H···O(11) [$1-x$, $-^1/_2 + y$, $-z$] with geometries O(9)···O(11) = 2.846 (2) Å, O(11)···H = 2.01 (4) Å, and angle O(9)–H–O(11) = 162 (2)°.

Biological Activity. The new briarein type compounds were not cytotoxic against P-388 leukemia cells. However, some of the briareolides displayed potential as antiinflammatory agents. At a dose of 50 μg/ear, briareolides A (10), B (11), C (12), D (13), and E (14) exhibited 71%, 55%, 75%, 85%, and 46% inhibition of inflammation, respectively, in the mouse ear assay.[26]

Summary. The diterpenes from *E. caribaeorum* (erythrolides) possess certain structural features so far unreported in the literature for compounds of this type. Erythrolides C (3), D (4), and H (5) have a 2*R**,3*R**-epoxide moiety in the 10-membered ring while erythrolides E (6), F (7), I (8), and G (9) have an ether bridge across the 10-membered ring between C-2 and C-8. Erythrolides D (4) and F (7) contain an unusual acetoxyacetate group at C-9. All of the erythrolides, except erythrolide H (5), are chlorinated at the C-6 position. Erythrolide H is unique among the compounds in this series in having a C-5,6 double bond and a hydroxyl substituent at C-16 instead of an exocyclic C-5,11 double bond. Only one of the erythrolides, erythrolide G (9), does not possess an α,β-unsaturated ketone moiety.

In contrast, the nine new briarein derivatives (briareolides) isolated from *Briareum* sp. are all nonchlorinated and more highly oxygenated, typically possessing hydroxyl, butyrate, and/or acetate groups at positions C-2, C-9, C-11, C-12, and C-14. Only one briareolide (briareolide I, 18) has an α,β-unsaturated ketone functionality. All of the briareolides except briareolide G (16), which has an α,β-unsaturated γ-lactone, contain an α,β-epoxy γ-lactone, a feature found only in a few other briarane diterpenes isolated from *Briareum* spp.[12] Structural variations in the briareolide series occur mainly in the substitution around the six-membered ring: two briareolides (A and B, 10 and 11) are 11,12-diols; compounds 12 (briareolide C) and 13 (briareolide D) are 11,12-epoxy metabolites; compounds 14, 15, and 16 (briareolides E, F, and G) are 12-hydroxy briaranes; lastly, briareolide H (17) is a $\Delta^{11,12}$ compound.

Experimental Section[27]

Extraction and Isolation. *E. caribaeorum* collected in 1983 from the U.S. Virgin Islands and immediately frozen was freeze-dried (248 g dry weight) and then soaked sequentially in hexane (6 h), hexane (1 day), dichloromethane (1 day), and finally 1:1 chloroform-methanol (2 days). The solvents were evaporated in vacuo to yield ~400 mg of combined hexane extracts, 3.1 g of dichloromethane extract, and 5 g of chloroform–methanol (1:1) extract. The dichloromethane extract (extract C) was chromatographed extensively according to Scheme I to yield six compounds: the known diterpenes 1 and 2 and the new compounds 3–6. The hexane extracts obtained from *E. caribaeorum* collected in Jamaica were combined and chromatographed by using a Florisil column. The column fractions that gave a crystalline residue upon evaporation of the solvent were chromatographed further by HPLC in a manner analogous to that shown in Scheme I to yield compounds 1–9.

Scheme I. Chromatography Scheme for Extract C (CH_2Cl_2 Extract) of *E. caribaeorum*[a]

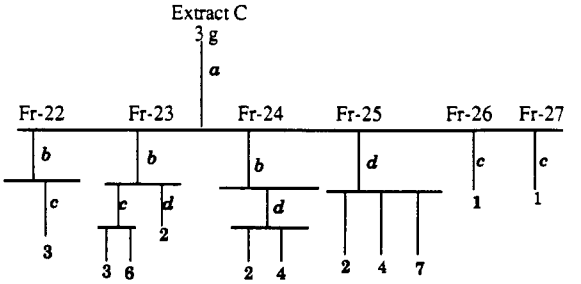

[a] (a) SiO_2 flash column chromatography, hexane with step increase in EtOAc, up to 50% EtOAc in Hexane. (b) SiO_2 flash column chromatography, $CHCl_3$ with step increase in MeOH, up to 20% MeOH in $CHCl_3$. (c) SiO_2 HPLC, acetone–hexane (25:75). (d) Cyanopropyl bonded-phase HPLC, hexane–2-propanol (2:1).

The octocoral *Briareum* sp. was collected in Puerto Rico near La Parguera in 1986, immediately frozen and stored, and then freeze-dried after a few months of storage to give 500 g of dry animal tissue. This material was soaked sequentially in hexane (6 h), hexane (1 day), dichloromethane (1 day), and finally, chloroform–methanol (1:1) (2 days). Evaporation of the solvents under vacuum yielded 5 g of combined hexane extract (A), 6.8 g of dichloromethane extract (B), and 9.6 g of chloroform–methanol (1:1) extract (C). Extract C was dissolved in 250 mL of methanol, about 150 mL of water was added, and the resulting solution was then extracted with ethyl acetate (2 × 200 mL). After evaporation of the ethyl acetate under vacuum, the residual extract was dissolved in 250 mL of methanol. The methanol solution was then extracted with hexane (2 × 200 mL). Upon separation of the layers and evaporation of the solvents, the methanol layer yielded 2.5 g of material designated as fraction C-1. The dichloromethane extract (extract B) was chromatographed extensively in a manner similar to that shown in Scheme I to yield compounds 1, 2, 4, and the new compounds 10–15, 17, and 18. Chromatography of fraction C-1 resulted in the isolation of more of these new compounds and a ninth compound, 16.

Erythrolide A (1): ~15 mg; white powder; ^1H NMR ($CDCl_3$, 300 MHz) δ 6.44 (1 H, dddd, 16.0, 7.1, 1.0, 1.0), 6.02 (1 H, dd, 1.0, 3.0), 5.87 (1 H, ddd, 16.6, 2.6, 1.0), 5.62 (1 H, s), 5.49 (1 H, s), 5.45 (1 H, 1.8), 5.16 (1 H, d, 9.5), 4.57 (1 H, d, 9.5), 3.40 (1 H, br s),

(26) Antiflammatory activity testing was carried out by Dr. R. S. Jacobs's group, University of California, Santa Barbara.

(27) General experimental conditions were as described earlier: Pordesimo, E. O.; Schmitz, F. J. *J. Org. Chem.*, in press.

3.18 (1 H, q, 7.2), 2.97 (1 H, br s), 2.23 (3 H, s), 2.14 (3 H, s), 2.01 (3 H, s), 1.98 (1 H, d, 10.2), 1.58 (3 H, s), 1.38 (3 H, s), 1.34 (1 H, dddd, 10.2, 7.3, 1.0), 1.21 (3 H, d, 7.0).

Erythrolide B (2): ~200 mg; colorless foam; $C_{26}H_{31}O_{10}Cl$; UV (MeOH) λ_{max} 215; ^1H and ^{13}C NMR data in Tables I and III.

Erythrolide C (3): 65 mg; white powder from slow evaporation of acetone–hexane solution; $C_{24}H_{29}O_9Cl$; mp 125–129 °C; UV (MeOH) λ_{max} 215 (ϵ 8910); IR (film on NaCl plate) 3540, 1780, 1735, 1685, 1225 cm^{-1}; low-resolution MS (EI$^+$, 12 eV) m/z (relative intensity) 461 (3.8), 402 (2.5), 401 (8.3), 394 (3.0), 342 (2.5), 341 (8.8), 323 (3.0), 206 (58), 164 (64), 147 (58), 135 (100); low-resolution (FAB$^+$) m/z (relative intensity) 499 [39.4, (M + H)$^+$ + 2)], 497 [100, (M + H)$^+$], 437 (29.5), 439 (13.2); high-resolution FAB$^+$ MS found (M + H)$^+$ 497.1545, calcd 497.1578; ^1H and ^{13}C NMR data in Tables I and III.

Erythrolide D (4): 80 mg; white powder from slow evaporation of acetone–hexane solution; $C_{26}H_{31}O_{11}Cl$; mp 120–122 °C; UV (MeOH) λ_{max} 216 (ϵ 6874); IR (film on NaCl plate) 3540, 3020, 1775, 1745, 1685, 1235 cm^{-1}; low-resolution MS (EI$^+$, 12 eV) m/z (relative intensity) 519 (1.5, M$^+$ – Cl), 495 (0.9), 479 (1.3), 459 (4.5), 394 (2.2), 358 (1.0), 377 (1.2), 341 (3.9), 101 (100); high-resolution MS (FAB$^+$) m/z 577.1453 [(M + Na)$^+$], calcd 577.1453; ^1H and ^{13}C NMR data in Tables I and III.

Erythrolide H (5): 6.1 mg; colorless foam; $C_{24}H_{30}O_{10}$; UV (MeOH) λ_{max} 217 (ϵ 7570); IR (film on NaCl plate) 3440, 3020, 1770, 1740, 1685, 1220 cm^{-1}; low-resolution MS (EI$^+$, 12 eV) m/z (relative intensity) 460 (1.6, M$^+$ – H_2O), 400 (1.7, M$^+$ – AcOH), 372 (1.2), 340 (1.7), 247 (13.4), 193 (23.1), 175 (11.7), 164 (16.3), 122 (100); ^1H and ^{13}C NMR data in Tables I and III.

Erythrolide E (6): ~300 mg; white powder from evaporation of acetone–hexane solution; mp 128–129 °C; $C_{24}H_{29}O_9Cl$; UV (MeOH) λ_{max} 216 nm (ϵ 5490); IR (film on NaCl plate) 3480, 1770, 1740, 1685, 1210 cm^{-1}; low-resolution MS (EI$^+$, 12 eV) m/z (relative intensity) 498 (0.8), 496 (2.6), 461 (1.0), 446 (1.6), 439 (1.3), 437 (3.7), 421 (8.8), 394 (9.9), 135 (100); high-resolution EI$^+$ MS, M$^+$ observed 496.1480, calcd 496.150; ^1H and ^{13}C NMR data in Tables II and III.

Erythrolide F (7): ~300 mg; white powder from evaporation of acetone–hexane solution; mp 118–119 °C; $C_{26}H_{31}O_{11}Cl$; UV (MeOH) λ_{max} 218 (ϵ 5194); IR (film on NaCl plate) 3470, 2940, 2900, 2830, 1770, 1735, 1675, 1360, 1225 cm^{-1}; high-resolution EI$^+$ MS, m/z (relative intensity) 556.1459 (1.0, M$^+$ + 2), 554.1547 (1.2, M$^+$), 495.1404 (2.3), 479.1129 (7.8), 394.1214 (5.4), 101.0033 (100); ^1H and ^{13}C NMR data in Tables II and III.

Erythrolide I (8): 5.5 mg; whitish film; $C_{24}H_{29}O_{10}Cl$; UV (MeOH) λ_{max} 221 (ϵ 11 690); IR (film on NaCl plate) 3740, 1770, 1736, 1697, 1686, 1651 cm^{-1}; low-resolution MS (EI$^+$, 70 eV) m/z (relative intensity) 512 (1.5, M$^+$), 477 (1.0), 453 (2.4), 439 (2.0), 437 (6.0), 394 (3.2), 135 (100), 77 (26.6); high-resolution MS (FAB) m/z 513.1500 (M + H)$^+$, calcd for $C_{24}H_{30}O_{10}{}^{35}Cl$ 513.1527; ^1H and ^{13}C NMR data in Tables II and III.

Erythrolide G (9): 5 mg; whitish film; $C_{26}H_{33}O_{10}Cl$; IR (film on NaCl plate) 3480, 3020, 1785, 1745, 1640, 1370, 1245, 1220 cm^{-1}; low-resolution MS (EI$^+$, 12 eV) m/z (relative intensity) 540 (1.5, M$^+$), 483 (2.1), 481 (7.2, M$^+$ – OAc), 405 (1.5), 385 (2.2), 326 (2.7), 325 (9.4), 190 (100); high-resolution MS (FAB) m/z 563.1688 [(M + Na)], calcd for $C_{26}H_{33}O_{10}{}^{35}ClNa$ 563.1660; ^1H and ^{13}C NMR data in Tables II and III.

Acetate of Erythrolide E (19). Erythrolide E (6) (1.0 mg) was stirred with 0.5 mL of acetic anhydride in 0.5 mL of pyridine for 24 h at room temperature. After evaporation of excess reagent under nitrogen, the residue was chromatographed by HPLC on silica gel (acetone–hexane, 15:85) to give pure erythrolide E acetate (19) in quantitative yield: ^1H NMR ($CDCl_3$, 300 MHz) δ 6.83 (1 H, d, 10.1), 6.03 (1 H, d, 10.1), 5.66 (1 H, br s), 5.59 (1 H, s), 5.36 (1 H, s), 5.19 (1 H, m), 4.78 (1 H, d, <1), 4.38 (1 H, d, <1), 4.14 (1 H, d, 3.2), 3.20 (1 H, d, 1.8), 2.78 (1 H, dd, 14.8, 4.6), 2.56 (2 H, m), 2.26 (3 H, s, OAc), 2.11 (3 H, s, OAc), 2.05 (3 H, s, OAc), 1.56 (3 H, s), 1.46 (3 H, s), 1.06 (3 H, d, 7.05).

Acetate of Erythrolide F (20). According to the above procedure, erythrolide F (7) (2.0 mg) was acetylated and the product purified to give 20 in quantitative yield: ^1H NMR ($CDCl_3$, 300 MHz) δ 6.82 (1 H, d, 10.1), 6.03 (1 H, d, 10.1), 5.72 (1 H, br s), 5.60 (1 H, br s), 5.37 (1 H, br s), 5.17 (1 H, m), 4.78 (1 H, d, <1), 4.71 (2 H, s), 4.43 (1 H, d, 1.7), 4.16 (1 H, d, 3.7), 3.24 (1 H, br s), 2.81 (1 H, dd, 15.0, 5.4), 2.51 (2 H, m), 2.21 (3 H, s, OAc), 2.12 (3 H, s, OAc), 2.11 (3 H, s, OAc), 1.52 (3 H, s), 1.47 (3 H, s), 1.11 (3 H, d, 7.2).

Acetate of Erythrolide I (20). The reaction was carried out as in acetylation of 7 with 1.5 mg of erythrolide I (8). Purification of the product by HPLC on silica gel led to the isolation of pure erythrolide F acetate (20).

Briareolide A (10): ~350 mg; colorless needles from evaporation of acetone–hexane solution; mp 242–243 °C dec; $C_{28}H_{40}O_{11}$; IR (film on NaCl plate) 3460, 1775, 1760, 1730, 1700, 1280 cm^{-1}; low-resolution MS (EI$^+$, 12 eV) m/z (relative intensity) 552 (1.2), 465 (4.3), 464 (5.3), 404 (12.5), 362 (12), 361 (13), 344 (19.5), 326 (13), 273 (35), 256 (46), 255 (42), 201 (42), 185 (100); high-resolution FAB$^+$ MS m/z (formula) 553.2674 ($C_{28}H_{41}O_{11}$, M$^+$ + H), 575.2478 ($C_{28}H_{40}O_{11}Na$, M$^+$ + Na); ^1H and ^{13}C NMR data in Tables V and VII.

Briareolide B (11): ~200 mg; colorless needles, recrystallized from acetone–hexane; mp 249–250 °C; $C_{26}H_{36}O_{11}$; IR (film on NaCl plate) 3522, 1778, 1736, 1258 cm^{-1}; low-resolution MS (EI$^+$, 12 eV) m/z (relative intensity) 525 (3.7), 524 (9.8), 506 (1.3), 482 (1.6), 464 (9.8), 404 (23), 362 (22), 361 (25), 344 (34), 326 (25), 283 (43), 274 (67), 227 (65), 213 (73), 185 (100); high-resolution FAB$^+$ MS m/z (formula) 525.2392 [$C_{26}H_{37}O_{11}$, (M + H)$^+$], 547.2155 [$C_{26}H_{36}O_{11}Na$, (M + Na)$^+$; ^1H and ^{13}C NMR date in Tables V and VII.

Briareolide C (12): 85 mg; white powder from evaporation of acetone–hexane solution; $C_{28}H_{39}O_{10}$; mp 139–140 °C; IR (film on NaCl plate) 1780, 1760, 1730, 1250 cm^{-1}; low-resolution MS (FAB$^+$) m/z (relative intensity) 492 (2.3, M$^+$ – C_3H_6), 475 (5.9, M$^+$ – OAc), 474 (5.4, M$^+$ – AcOH), 447 (7.6), 446 (12.5), 387 (17.6), 386 (31.7), 327 (17.8), 326 (22), 311 (13), 256 (95.7), 255 (100); high-resolution MS (FAB$^+$) m/z (formula) 535.2593 [$C_{28}H_{39}O_{10}$, (M + H)$^+$], 557.2363 [$C_{28}H_{39}O_{10}Na$, (M + Na)$^+$]; ^1H and ^{13}C NMR data in Tables V and VII.

Briareolide D (13): 10 mg; colorless film; $C_{26}H_{34}O_{10}$; IR (film on NaCl plate) 1782, 1735, 1254 cm^{-1}; low-resolution MS (EI$^+$, 12 eV) m/z (relative intensity) 464 (4.1, M$^+$ – CH_2CO), 447 (9.8), 446 (13.4), 404 (82.3), 403 (100), 387 (46.8), 386 (85); high-resolution MS (FAB$^+$) (M + H)$^+$ found m/z 507.2196, calcd 507.2230; ^1H and ^{13}C NMR data in Tables V and VII.

Briareolide E (14): 40 mg; colorless foam; $C_{28}H_{40}O_{10}$; mp 182–183 °C dec; IR (film on NaCl plate) 3560, 1782, 1760, 1732 cm^{-1}; low-resolution MS (EI$^+$, 12 eV) m/z (relative intensity) 448 (6.9, M$^+$ – $CH_3CH_2CH_2COOH$), 430 (6.5), 370 (18.4), 328 (32.3), 310 (45), 258 (93.6), 257 (60.7), 240 (100); high-resolution MS (FAB$^+$) (M + H)$^+$ found m/z 537.2696, calcd 537.2700; ^1H and ^{13}C NMR data in Tables VI and VIII.

Briareolide F (15): 15 mg; colorless foam; $C_{26}H_{36}O_{10}$; IR (film on NaCl plate) 3568, 3020, 1782, 1735, 1258 cm^{-1}; low-resolution MS (EI$^+$, 12 eV) m/z (relative intensity) 448 (4.2, M$^+$ – AcOH), 430 (4.2), 370 (12), 328 (25), 310 (34), 258 (92.7), 257 (64.1), 240 (100); high-resolution MS (FAB$^+$) m/z 508.2314 (M$^+$), calcd 508.2308; ^1H and ^{13}C NMR data in Tables VI and VIII.

Briareolide G (16): 5 mg; white powder from methanol–water; $C_{28}H_{40}O_9$; UV (MeOH) λ_{max} 204 (ϵ 9020); IR (film on NaCl plate) 3530, 1748, 1736, 1373, 1230 cm^{-1}; low-resolution MS (EI$^+$, 12 eV) m/z (relative intensity) 460 (4.5, M$^+$ – HOAc), 432 (3.6, M$^+$ – $CH_3CH_2CH_2COOH$), 372 (27.8), 312 (73.8), 294 (100); low-resolution MS (FAB$^+$) m/z (relative intensity) 543 [14.7, (M + Na)$^+$], 521 [6.4, (M + H)$^+$, 433 (7.3), 391 (9.8); high-resolution MS (FAB$^+$) m/z 521.2732, calcd from $C_{28}H_{41}O_9$ (M + H)$^+$ 521.2751; ^1H and ^{13}C NMR data in Tables VI and VIII.

Briareolide H (17): 3 mg; colorless film; IR (film on NaCl plate) 1782, 1760, 1736, 1250 cm^{-1}; high-resolution MS (FAB$^+$) m/z 513.2090, calcd for $C_{26}H_{34}O_9Na$ 513.2101; ^1H and ^{13}C NMR data in Tables VI and VIII.

Briareolide I (18): 2.5 mg; colorless film; UV (MeOH) λ_{max} 217 (ϵ 5614); IR (film on NaCl plate) 1782, 1735, 1682 cm^{-1}; low-resolution MS (FAB$^+$, 70 eV) m/e (relative intensity) 474 (19, M$^+$), 404 (100), 403 (3), 387 (11), 386 (12), 344 (34), 291 (66), 256 (53), 240 (46); high-resolution MS (FAB$^+$) m/z 497.2178, calcd for $C_{26}H_{34}O_8Na$ 497.2151; ^1H and ^{13}C NMR data in Tables VI and VIII.

X-ray Experimental Results. A plate-shaped crystal of 11 of size 0.70 × 0.36 × 0.05 mm was selected for all crystallographic measurements. Cell dimensions were obtained by least-squares fit to $\pm 2\theta$ values of 48 reflections measured at 163 K using Cu

Table XII. Calculated and Observed Bijvoet Differences

h	k	l	ESF[a] obsd	ESF[a] calcd
$\bar{3}$	2	3	2.70	2.11
2	1	2	2.68	2.04
9	9	0	-0.34	-1.81
$\bar{1}$	4	1	-0.99	-1.64
1	5	4	2.66	1.63
$\bar{8}$	2	5	-0.81	-1.52
1	7	5	1.48	1.50
1	5	3	-0.20	-1.45
3	5	9	-1.63	-1.42
$\bar{11}$	7	6	-0.23	-1.42
11	6	2	-0.58	-1.37
$\bar{3}$	10	1	1.13	1.37
$\bar{13}$	1	6	-2.06	-1.37
$\bar{9}$	7	6	2.64	1.36
2	3	4	2.82	1.35
0	10	0	0.74	1.34
$\bar{1}$	8	8	-1.14	-1.30
0	12	0	1.33	1.27
$\bar{1}$	7	8	-0.44	-1.23
2	9	0	2.28	1.22
6	5	2	-0.07	-1.21
$\bar{6}$	3	4	3.49	1.21
$\bar{3}$	3	2	-0.38	-1.20
7	4	0	1.43	1.17

[a] ESF = $[F^2(+) - F^2(-)]/\sigma(F^2)$, where $F^2(+) = F^2(hkl)$ and $F^2(-) = F^2(h\bar{k}\bar{l})$.

$K\alpha_1$ radiation. All X-ray measurements were carried out on an Enraf-Nonius CAD-4 diffractometer equipped with a liquid N_2 low-temperature device.

Crystal data: briareolide B, $C_{26}H_{36}O_{11}$, M_r = 524.6, monoclinic, $P2_1$, a = 12.606 (2) Å, b = 10.460 (3) Å, c = 10.304 (2) Å, β = 107.68 (1)°; V = 1294.5 Å^3, Z = 2, D_{calcd} = 1.345 gm cm^{-3}, $F(000)$ = 560, μ(Cu Kα) = 7.9 cm^{-1}.

The intensity data of all the unique reflections within 2θ range 0-150° were collected at 163 ± 2 K by using Cu Kα radiation and a θ-2θ scan technique with a variable scan width of (0.90 + 0.20 tan θ)°. A total of 2818 unique reflections were recorded, of which 2771 reflections were considered "observed" on the basis of $I > 2\sigma(I)$. The intensities were corrected for Lorentz and polarization factors, but no absorption correction was made. The structure was solved by direct methods and the use of the program MULTAN80[28] and refined by a full-matrix least-squares routine SHELX86[29] in which the quantity $\sum w(F_o - F_c)^2$ is minimized, where $w = 1/\sigma^2(F_o)$. All the hydrogen atoms were located from a difference Fourier map, and their parameters were refined. The non-hydrogen atoms were given anisotropic thermal parameters. The refinement converged to a final R = 0.0295, R_w = 0.0363 for 2771 observed reflections [$I > 2\sigma(I)$], S = 1.4, Δ/σ 0.04, electron density in the final difference map ±0.2 e/Å^3. The absolute configuration of briareolide B was determined by a Bijvoet method[30,31] using the anomalous dispersion of Cu radiation by oxygen and carbon atoms. Intensities of 24 most enantiomer sensitive Friedel pairs were measured repeatedly (15 times each) at low temperature. The calculated and observed weighted Bijvoet differences for these pairs of reflections are compared in Table XII. The intensity differences of all 24 pairs are in agreement with the absolute configuration shown in this report.

Acknowledgment. This work was supported by the Department of Commerce, NOAA Sea Grant Project NA86AA-D-SG074 to F.J.S., and NCI Grant CA-17562 to D.v.d.H. We thank Drs. S.A. Look and W. Fenical of Scripps Institute of Oceanography for providing NMR spectra of erythrolides A and B, Dr. F.M. Bayer of the Smithsonian Institute for identifying the gorgonians, and Dr. R. S. Jacobs's group, University of California, Santa Barbara, CA, for the antiinflammatory activity testing.

Supplementary Material Available: Bond distances, bond angles, torsion angles, hydrogen atom parameters, and anisotropic thermal parameters for 11 and ^{13}C NMR spectra of 3-14 and 16-18 (21 pages). Ordering information is given on any current masthead page.

(28) Main, P.; Fiske, S. J.; Hull, S. E.; Lessinger, L.; Germain, G.; Declerq, J.-P.; Woolfson, M. M. *MULTAN80. A System of Computer Programs for the Automatic Solution of Crystal Structures from X-ray Diffraction Data*; University of York: York, England, 1980.

(29) Sheldrick, G. M. *SHELX76. Program for Crystal Structure Determination*; University of Cambridge: Cambridge, England, 1986.

(30) Bijvoet, J. M.; Peerdeman, A. F.; van Bommel, A. J. *Nature* **1951**, *168*, 271.

(31) van der Helm, D.; Hossain, M. B. In *Patterson and Pattersons*; Glusker, J. P., Patterson, B. K., Rossi, M., Eds.; Oxford University Press: New York, 1987; p 482.

Biosynthetic Studies of Marine Lipids. 33.[1] Biosynthesis of Dinosterol, Peridinosterol, and Gorgosterol: Unusual Patterns of Bioalkylation in Dinoflagellate Sterols

José-Luis Giner and Carl Djerassi*

Department of Chemistry, Stanford University, Stanford, California 94305

Received September 5, 1990

The biosynthesis of the 23-methylated dinoflagellate sterols gorgosterol (**1-N**), dinosterol (**2-K**), and peridinosterol (**3-K**) was demonstrated experimentally using cell-free extracts of the dinoflagellates *Cryptothecodinium cohnii*, *Peridinium foliaceum*, and the cultured zooxanthella symbiont of *Cassiopea xamachana*. In assays of sterol methyltransferases using [^{3}H]-*S*-adenosylmethionine, radiochemical conversions were demonstrated by reverse phase HPLC of the Δ^{24} sterol side chain (**5**) to the 24-methylene side chain (**4**); of the sequence 24(*R*)-4α-methylergost-22-enol (**9-K**) to dinosterol (**2-K**) to 4α-methylgorgostanol (**1-K**); and, in *P. foliaceum*, of 24-(*R*)-4α-methylergost-22-enol (**9-K**) to peridinosterol (**3-K**). Methylation of the 24(*R*)-methyl Δ^{22} side chain (**9**) in *P. foliaceum* is believed to involve more than one SAM–sterol methyltransferase based on changes in the ratios of the products (**2** and **3**) with changes in the conditions of the assay. Furthermore, deuterium substitution of the sterol substrate (**9-K**) at C-23 did not significantly alter the product ratio. A hypothesis is put forward that the attenuation of gorgosterol (**1-N**) production in aposymbiotic zooxanthellae is linked to an increase in dimethylpropiothetin biosynthesis via a decrease in *S*-adenosylmethionine concentration.

Almost half a century has passed since the discovery of gorgosterol (**1-N**)[2] and 20 years since the elucidation of the structure of this unique cyclopropyl sterol[3] marked our entry into the field of marine sterol chemistry.[4] A bios-

0022-3263/91/1956-2357$02.50/0 © 1991 American Chemical Society